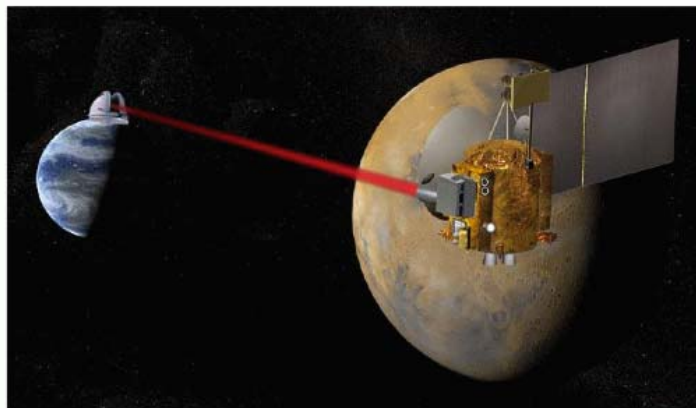




Fundamentals of Free-Space Optical Communication



Sam Dolinar, Bruce Moision, Baris Erkmen

*Jet Propulsion Laboratory
California Institute of Technology*

**Keck Institute for Space Studies (KISS) Workshop on
Quantum Communication, Sensing and Measurement in Space
Pasadena, CA – June 25, 2012**



Outline of the tutorial

- System diagram and link budgets
- System elements and the deep-space communication channel
- Fundamental capacity limits
- Coding to approach capacity
- Poisson-modeled noises
- + Other losses at the detector
- Atmospheric effects on optical communication
- Conclusions

- This talk will deal primarily with optical communication system design and analysis for *JPL's deep-space applications*. Free-space optical communication also has extensive application to near-Earth links, to space-space or space-Earth networks, and to terrestrial links and networks, but these will not be covered in this talk.



System diagram & link budgets



In this section, we discuss:

- **Basic comparison of link budgets for optical vs RF systems**
- **Block diagram of an optical communication system**
- **Detailed link budget including losses affecting optical links**
- **Example of a Mars-Earth optical link**

Coherent Microwave (RF) vs. Non-Coherent Infrared (Optical)

Received power

$$P_r = P_w \left(\frac{\pi D_t}{\lambda} \right)^2 \left(\frac{\pi D_r}{\lambda} \right)^2 \left(\frac{\lambda}{4\pi R} \right)^2 \eta$$

Ka-band Link

f	carrier frequency	32.0 GHz
D_t	transmit diameter	3.0 m
D_r	receiver diameter	34.0 m
η	system efficiency	-10.88 dB
N_o	noise spectral density	-178.45 dB-mW/Hz
W	bandwidth	500 MHz
P_t	transmit power	35 W

Capacity: supportable data rate ($P_r \gg P_w$ average power limited)

$$C_{OPT} \approx \frac{P_r \log_2 M}{(hc/\lambda)} \text{ b/s} \quad C_{RF} \approx \frac{P_r}{\ln(2)N_0} \text{ b/s}$$

Near-Infrared Link

λ	wavelength	1.55 μm
D_t	transmit diameter	22.0 cm
D_r	receiver diameter	11.8 m
η	system efficiency	-16.74 dB
α_b	noise spatial density	1.0 pW/m ²
T_s	slot width	0.5 ns
P_t	transmit power	4 W

$$\frac{C_{OPT}}{C_{RF}} \approx \left(\frac{D_t^o D_r^o}{D_t^r D_r^r} \right)^2 \left(\frac{\eta^o}{\eta^r} \right) \left(\frac{N_0}{(hc/\lambda)/\log_2(M)} \right) \left(\frac{\lambda^o}{\lambda^r} \right)^2$$

But gains are less in background noise, with pointing losses, etc.

aperture
-33 dB

efficiency
-16 dB

'noise'
-12 dB

beam divergence
+76 dB

= net 15 dB gain!

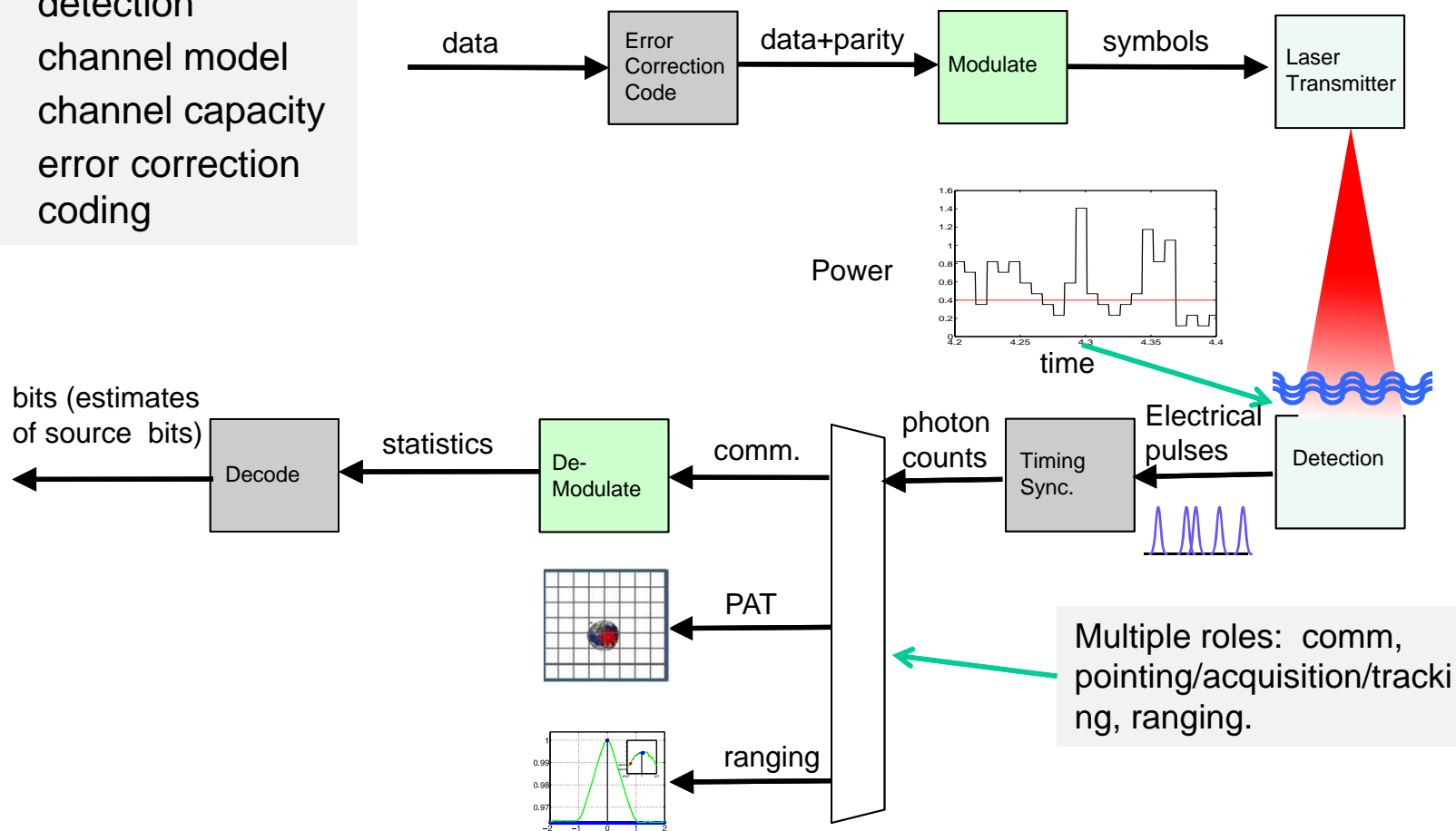
Capacity comparisons to answer the question: why optical?



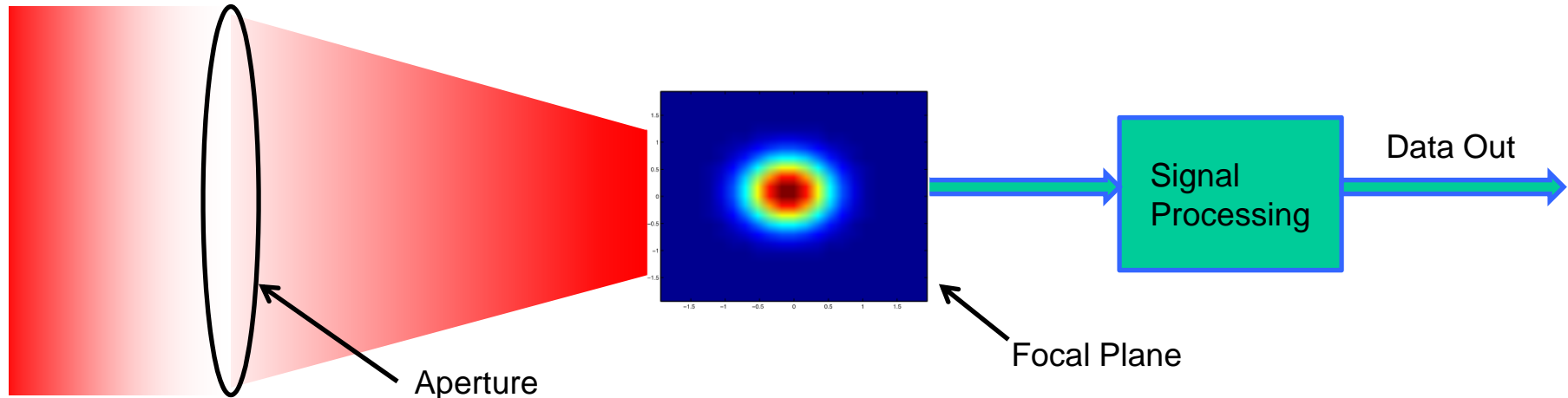
Block diagram of an optical communication system

To accurately assess system performance, we must consider the context (free-space communication link) and also specify various elements of the system and the channel:

- modulation
- detection
- channel model
- channel capacity
- error correction coding



Optical system link analysis accounting for losses



- Losses due to non-ideal system components (labeled efficiencies)
- Loss due to receiving the signal power in the presence of noise
- Losses due to spatial and temporal distortion of the of the received power

Received Power: average signal power received (in focal plane)

$$P_{rx} = P_t G_t G_r L_s L_a \eta_{pt} \eta_t \eta_r$$

- Transmitted power
- Transmit & Receive aperture gains
- Space loss
- Atmospheric loss
- Pointing loss
- Transmit & Receive efficiencies

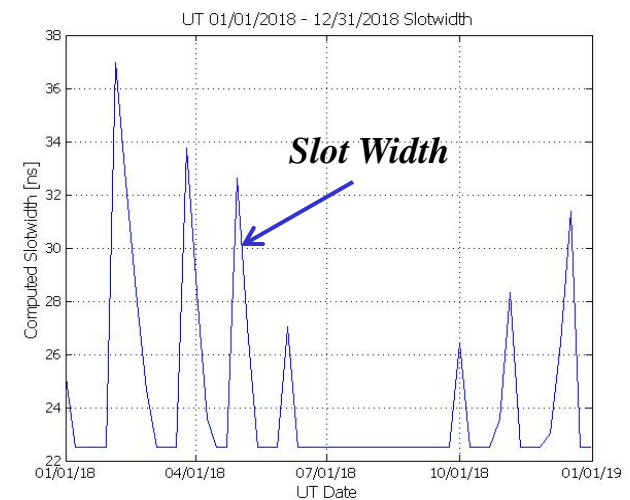
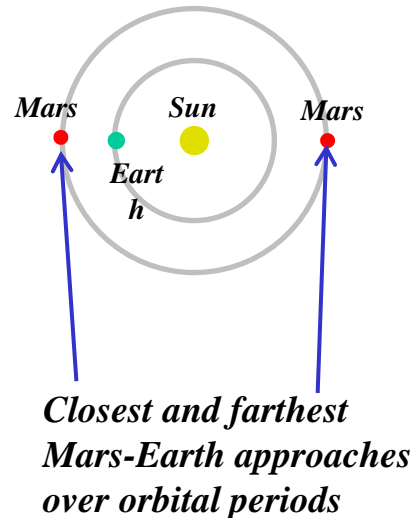
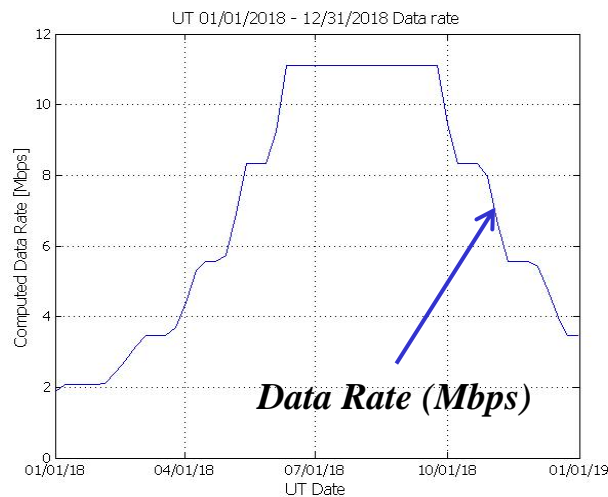
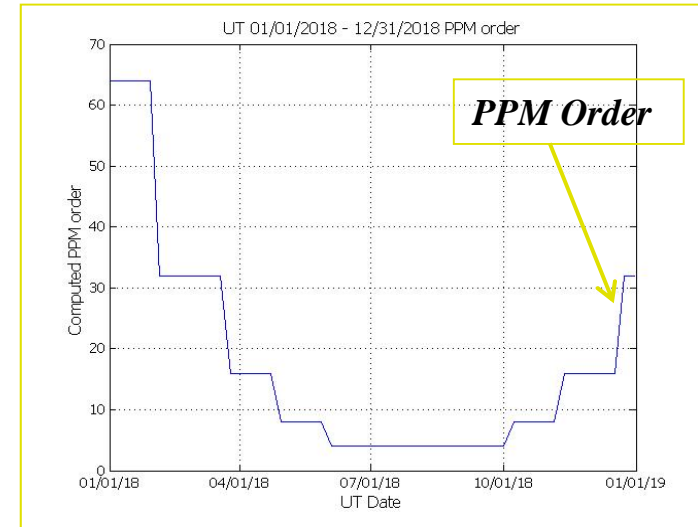
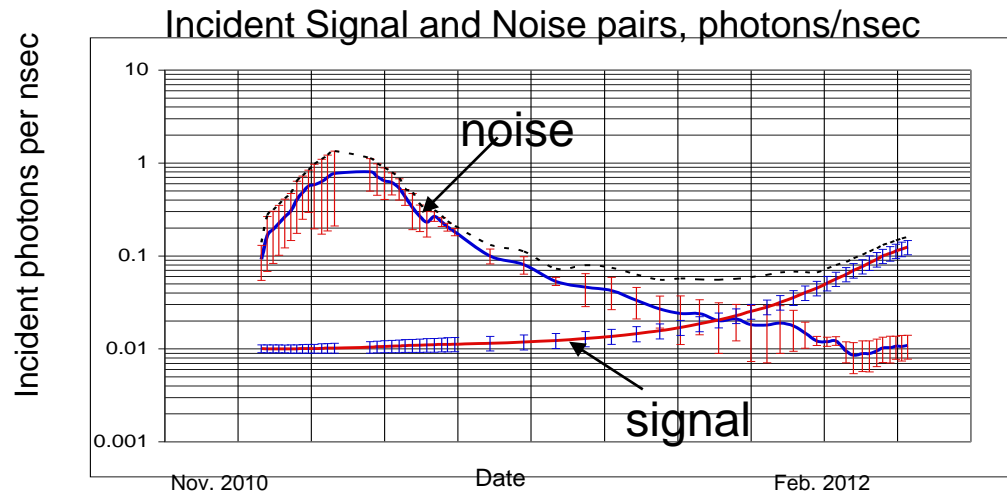
Required Power: required signal power in focal plane to support specified data rate

$$P_{rqd} = P_i / L_b L_j L_f L_t \eta_{det} \eta_{imp} \eta_{code} \eta_{int}$$

- Minimum (ideal receiver) required power
- Detector Blocking, Jitter & Efficiency losses
- Scintillation loss
- Truncation loss
- Implementation efficiency
- Code & Interleaver efficiencies

Example of Mars-Earth Link Received Signal and Noise Powers

- Wide range of operating points: 20 dB range of noise power, 12 dB range of signal power, due to changes in geometry (range, sun-earth-planet angle, zenith angle) and atmosphere.





System elements and the deep-space communication channel

In this section, we discuss:

- **The detection method (coherent or non-coherent)**
- **Intensity modulations for non-coherent detection**
- **Photon-counting channel model for intensity modulations**
- **Processing the observed photon counts to recover the data**



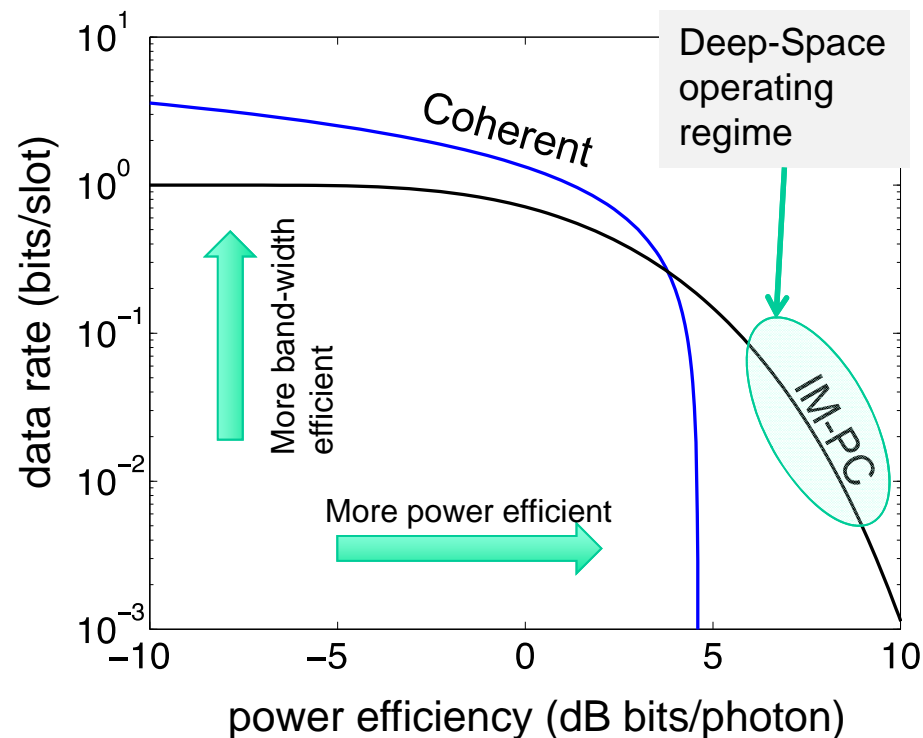
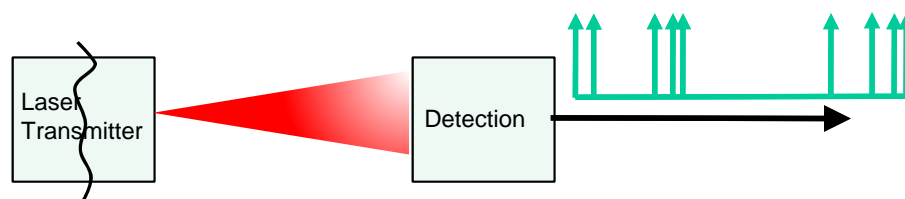
Optical signal detection methods

- **Coherent-detection**

- Enables, e.g., phase-modulations (BPSK).
- Requires correction of the phase front when transmitted through the turbulent atmospheric channel.

- **Non-coherent detection**

- Enables, e.g., intensity-modulation (IM)
- More power efficient at deep-space operating points (with low background noise).
- Photon-counting (PC) is practical.



IM-PC is near-optimal in our region of interest (low background noise, high power efficiency). In the remainder, we assume an IM-PC channel.

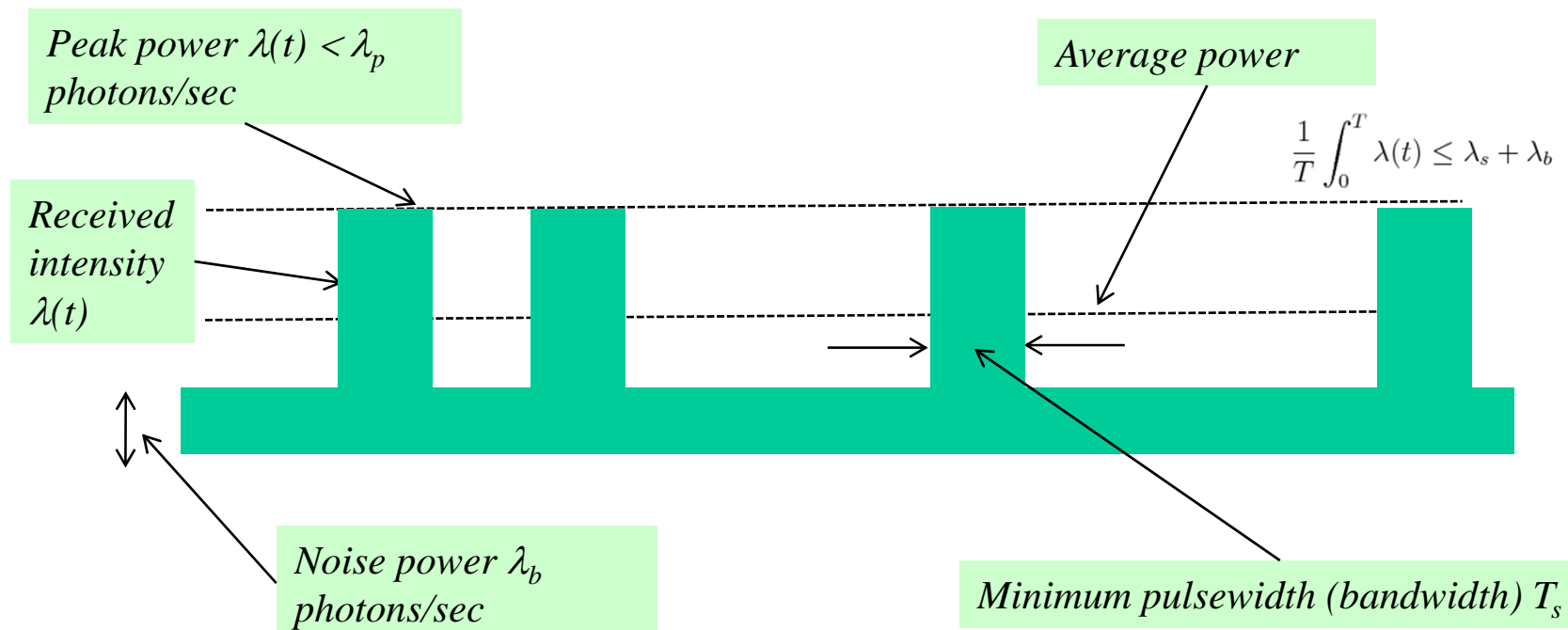


Coherent detection systems

- **Heterodyne** and **homodyne** receivers can be used with **arbitrary coherent-state modulations**.
- Such receivers, teamed with high-order modulations, achieve **much higher spectral efficiency** than PPM or OOK with photon counting.
 - Coherent detection systems are generally more practical than non-coherent systems for applications requiring **extremely high data rates**.
- Coherent systems also are practical for:
 - Systems that operate through the atmosphere
 - Systems limited by background noise or interference
 - Multiple-access applications
- However, coherent receivers encounter **brick-wall limits** on their maximum achievable **photon efficiencies**:
 - Maximum of 1 nat/photon (**1.44 bits/photon**) for heterodyning
 - Maximum of 2 nats/photon (**2.89 bits/photon**) for homodyning

Optical modulations for non-coherent detection

- Negligible loss in restricting waveforms to be *slotted* (change only at discrete intervals), and *binary* (take only two values)
 1. with no bandwidth (slotwidth) constraint [Wyner]
 2. in certain regions under a bandwidth constraint [Shamai]



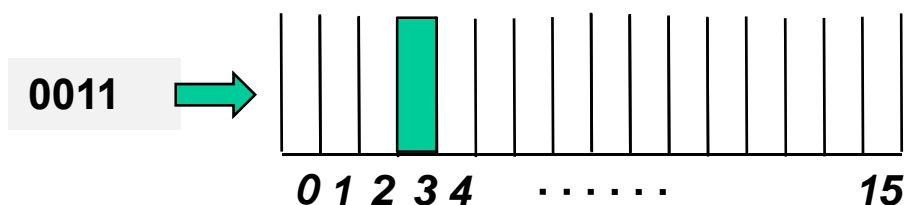


Optical modulations for non-coherent detection

Modulation: Collection of waveforms used to represent information

Pulse-Position-Modulation (PPM): $\log_2 M$ bits are represented by a single pulse out of M slots (here $M=16$).

On-Off-Keying (OOK): 1 bit is represented by a slot, which may either be occupied by a pulse or not.



- *Pulse-position-modulation (PPM) is an efficient way to implement a low duty cycle.*

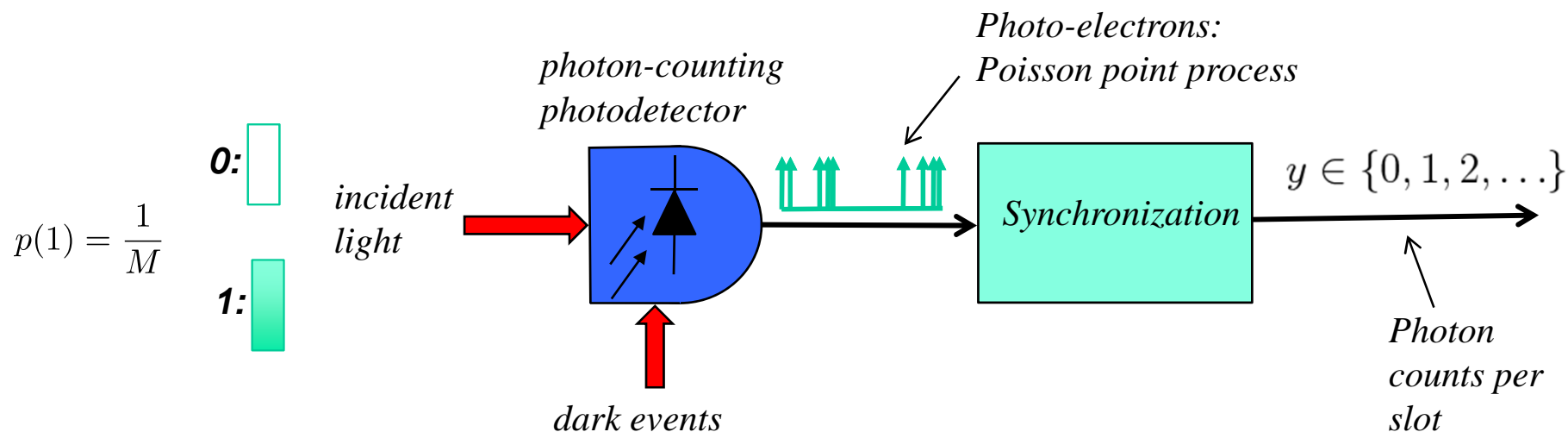
- *But for highest energy efficiency, **unpulsed OOK slots are much more probable than pulsed slots (low duty cycle).***

Given an optimum duty cycle $1/M$, how do we efficiently map an unconstrained binary sequence to a duty cycle $1/M$ sequence?

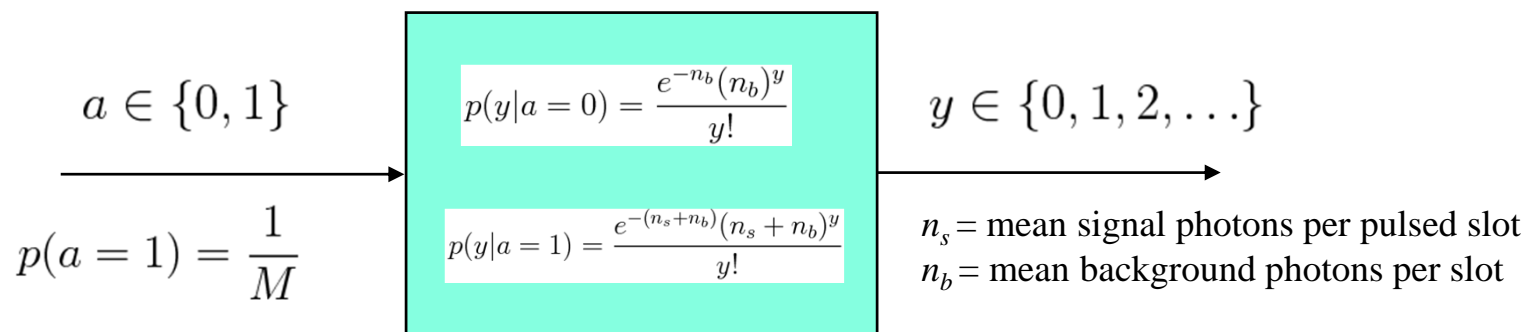
PPM is near-optimal over all possible modulations one could use on the intensity-modulated (IM) photon-counting (PC) channel in our region of interest (low duty-cycles).



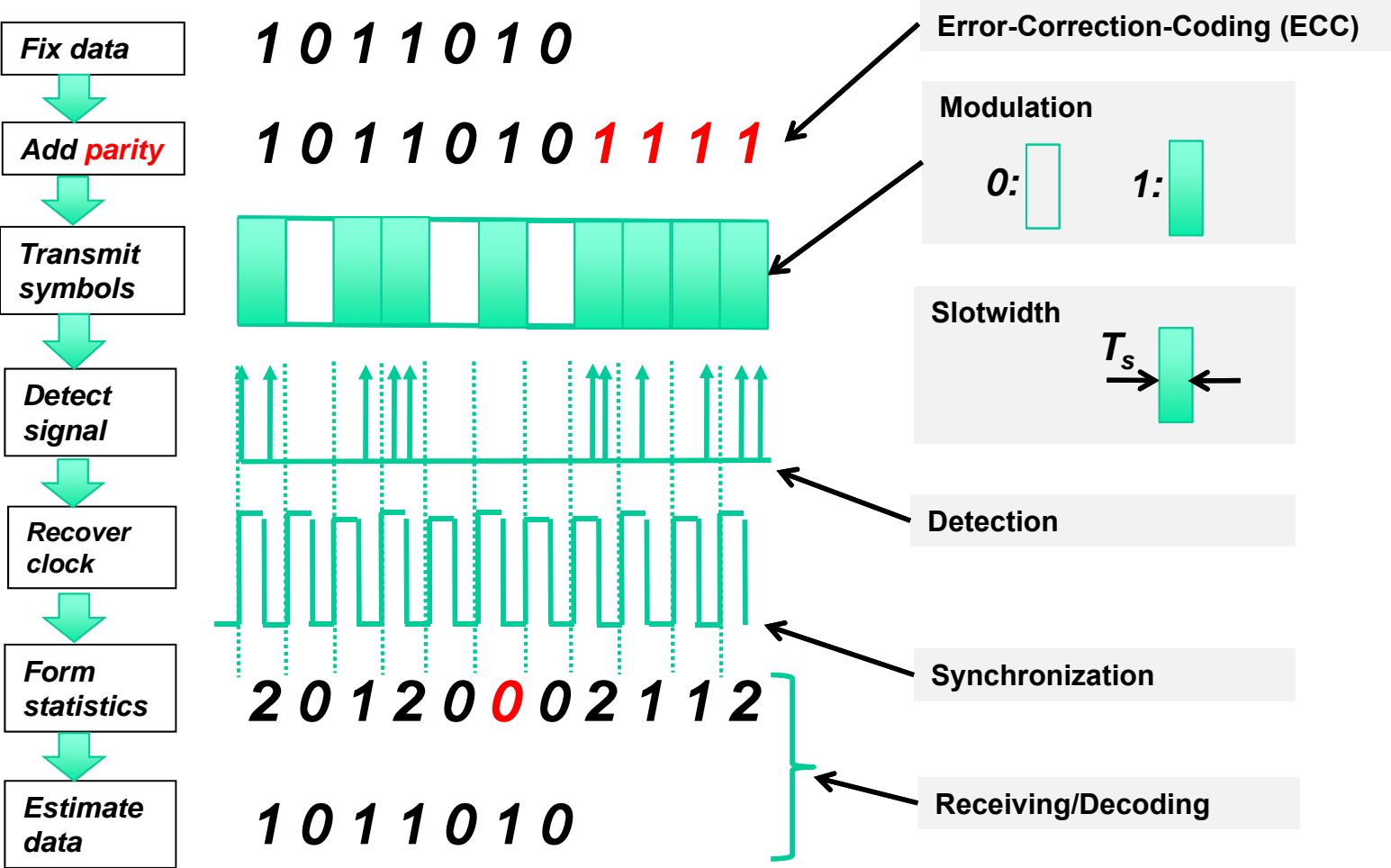
Intensity-modulated photon-counting channel model



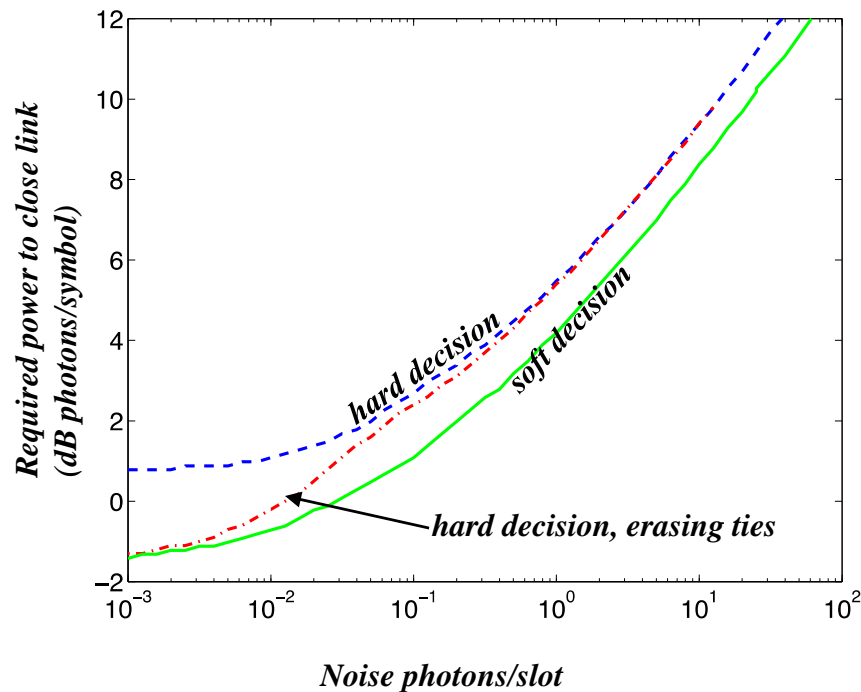
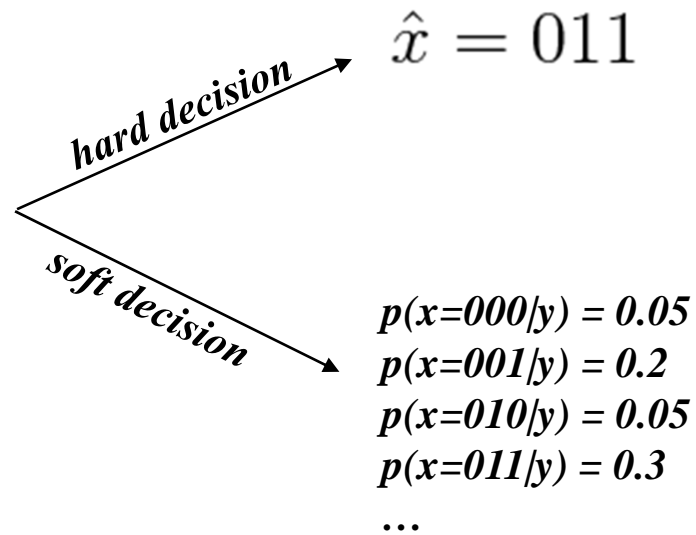
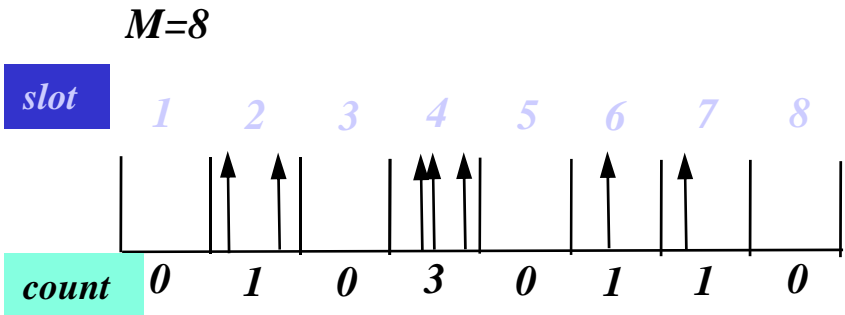
*Equivalent Channel model: Binary input, **Poisson**-distributed integer output*



Signal processing steps to communicate the data



Processing the photon counts: soft vs hard decisions



Capacity, hard and soft decisions
 $M = 16$, Average power to achieve
 $C = 1/8$ bits/slot

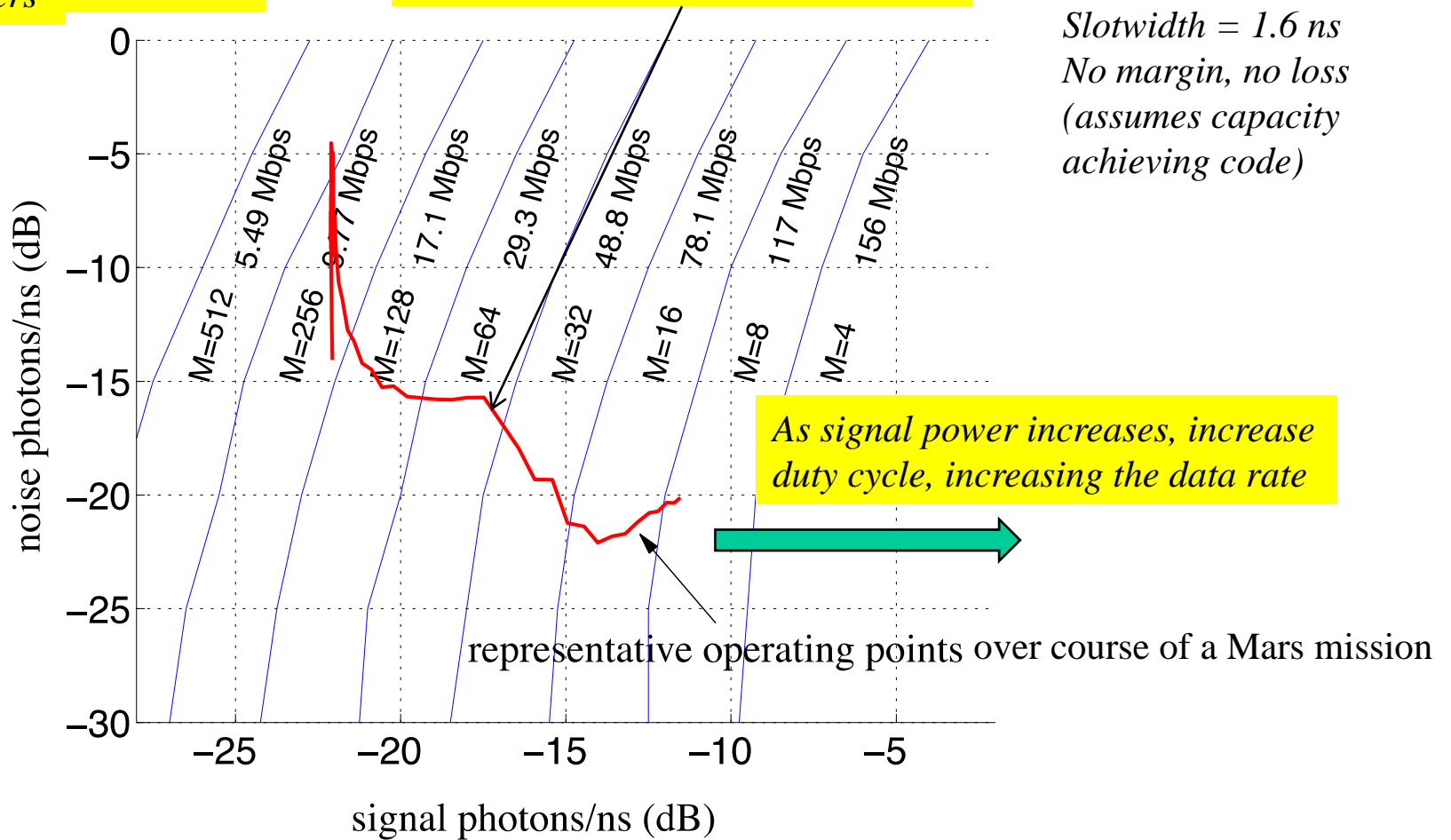
Typical region of operation is
 between 0.01 and 1.0 photons/slot

Near-optimal signaling for a deep-space link

Mapping of the received signal power, noise power plane to optimum PPM orders

Typical Earth-Mars link would ideally use many PPM orders

Slotwidth = 1.6 ns
No margin, no loss
(assumes capacity achieving code)





Fundamental capacity limits

In this section, we discuss:

- **Fundamental capacity limits for ideal noiseless quantum channel (i.e., only “quantum noise”).**
 - Limits for given combinations of modulation and receiver.
 - The ultimate limit (Holevo capacity) for any quantum-consistent measurement.
- **Capacity tradeoffs in terms of *dimensional information efficiency (DIE)* vs *photon information efficiency (PIE)*.**
 - PIE is measured in bits/photon.
 - DIE is measured in bits/dimension, bits/sec/Hz per spatial mode.
- **Alternative modulations/receivers to better approach the Holevo limit.**
- **Poisson model for noisy PPM or OOK channel capacity.**

Asymptotic Holevo capacity limit

- Asymptotically, for large photon efficiency, the ultimate (Holevo) capacity efficiencies are related by:

$c_d = \text{dimensional information efficiency (DIE)}$
[bits/dimension] or
[bits/s/Hz per spatial mode]

$c_d \rightarrow \tilde{c}_d^{(2)} \equiv e c_p 2^{-c_p}$

$c_p = \text{photon information efficiency (PIE)}$
[bits/photon]

- Thus, even at the ultimate limit, the dimensional efficiency (c_d) **must fall off exponentially** with increasing photon efficiency (c_p), except for a multiplicative factor proportional to c_p .

Asymptotic capacity of PPM and photon counting

- Asymptotically, for large photon efficiency, we have:

$$\log_2 M^* - c_p \rightarrow 0$$

$$c_d \rightarrow \tilde{c}_d^{(1)} \equiv \left(\frac{2}{e \ln 2} \right) 2^{-c_p} \approx 1.061 \times 2^{-c_p}$$

- Thus, with PPM and photon counting, and M optimized to achieve the best tradeoff, the dimensional information efficiency (c_d) must fall off exponentially with increasing photon efficiency (c_p).
- Comparing PPM + photon counting to the ultimate capacity, we obtain:

$$\frac{c_d(\text{ultimateHolevo})}{c_d(\text{PPM} + \text{counting})} \rightarrow \frac{\tilde{c}_d^{(2)}}{\tilde{c}_d^{(1)}} = \left(\frac{e^2 \ln 2}{2} \right) c_p \approx 2.561 c_p$$

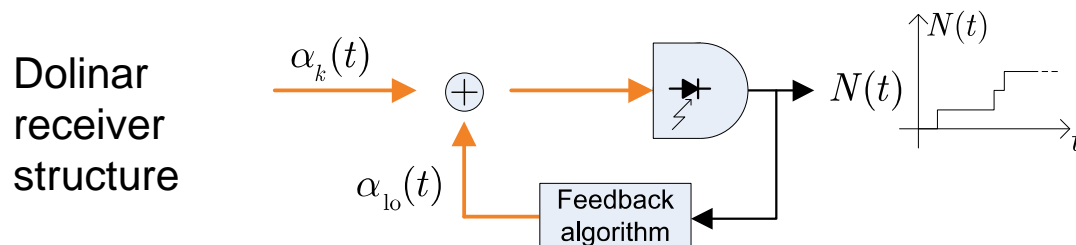
Can we approach Holevo capacity more closely than PPM/OOK + photon counting?

- Thus, the best possible factor by which the dimensional efficiency (c_d) can be improved by replacing a conventional system with PPM and photon counting with one that reaches the ultimate Holevo limit is only **linear in the photon efficiency** (c_p).

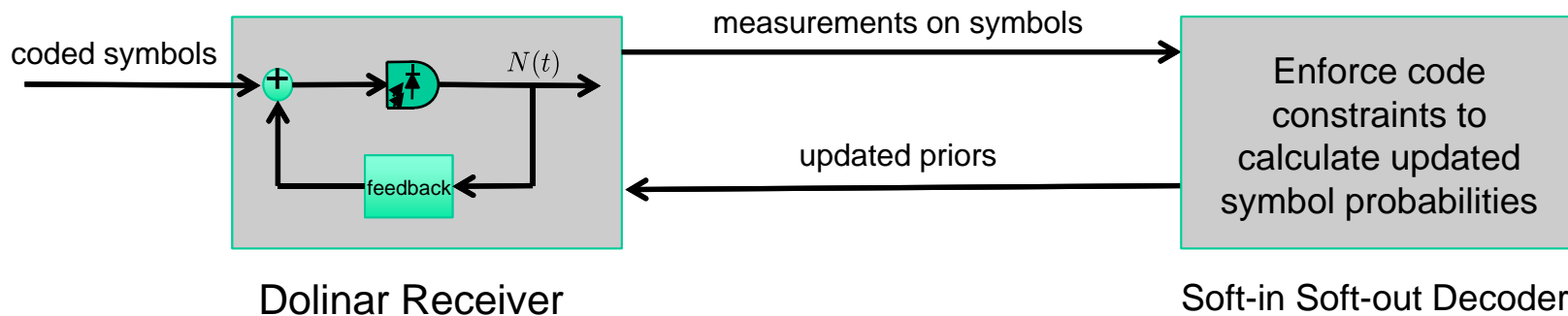


Dolinar receiver structure for BPSK or OOK

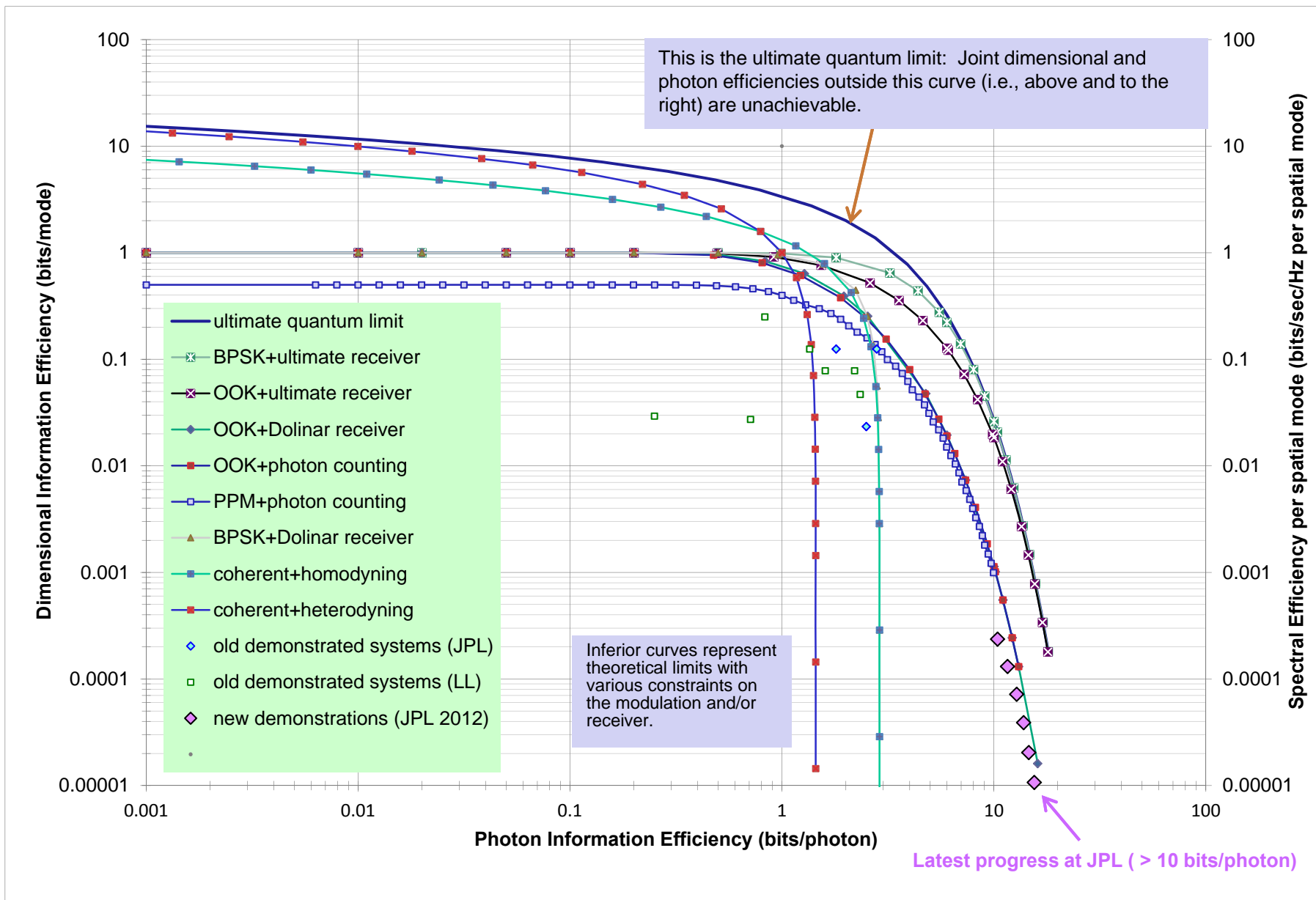
- The **Dolinar receiver** is known to be the optimal hard-decision measurement on an arbitrary binary coherent-state alphabet.
- It is also an optimal soft-decision measurement (at least for BPSK) for maximizing the mutual information.
- Unfortunately, **capacity improvements for OOK are minuscule** relative to photon counting, and there's still a **brick-wall upper limit of 2 nats/photon for BPSK**.



- The Dolinar receiver was extended to perform **adaptive measurements** on a **coded sequence** of binary coherent state symbols.
- There was **no capacity improvement** for the Dolinar receiver with adaptive priors.



Fundamental free-space capacity limits vs state-of-the-art optical systems



Communicating with single-photon number states

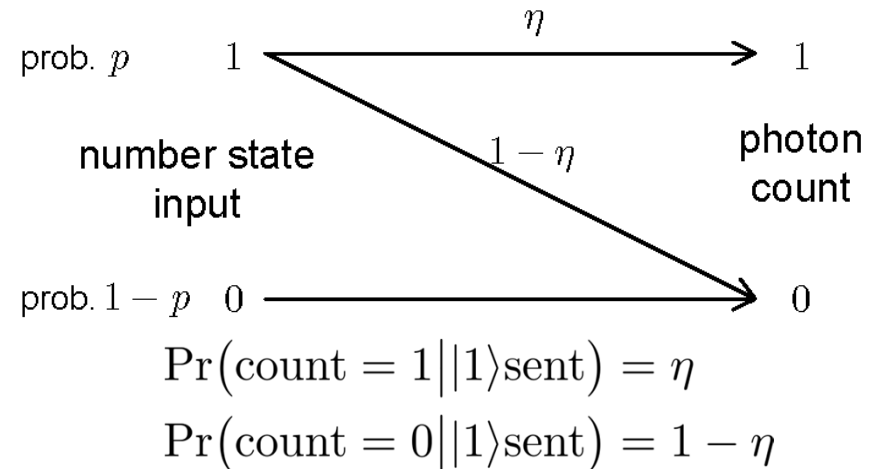
Can we do (significantly) better than than PPM/OOK + photon counting?

Yes, using quantum number states instead of coherent states.

Quantum-ideal number states:

- EM-wave with **deterministically observable energy**.
- Propagation is **degraded by channel transmissivity η** (i.e., the probability transmitted number-state photon is not received at detector).
- With ideal transmissivity, **number-states achieve Holevo limit** (with Bose-Einstein priors).
- **Binary number states are near-optimal** at large bits/photon (with ideal transmissivity).

Channel given by Z-channel of coherent-state OOK with $\epsilon \Leftrightarrow \eta$



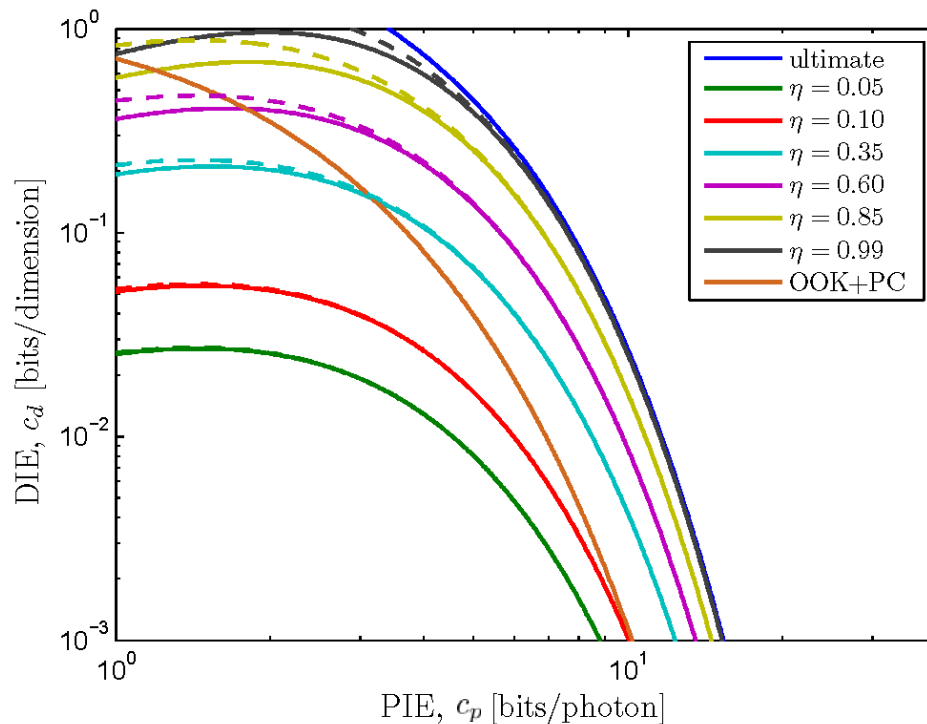
Asymptotic capacity of single-photon number states

- Asymptotically at high PIE, OOK with single-photon number states achieves:

$$c_d^{1\text{NS}}(c_p; \eta) \approx \underbrace{(e c_p 2^{-c_p})}_{\text{red bracket}} \underbrace{2^{-h_2(\eta)}}_{\text{red bracket}}$$

$$\left[\begin{array}{l} (1 - \eta)^{(1-\eta)} / e^{1-\eta} \text{ for } \eta \approx 1 \\ \eta/e \text{ for } \eta \ll 1 \end{array} \right]$$

$$c_d^{\text{Hol}}(c_p)$$

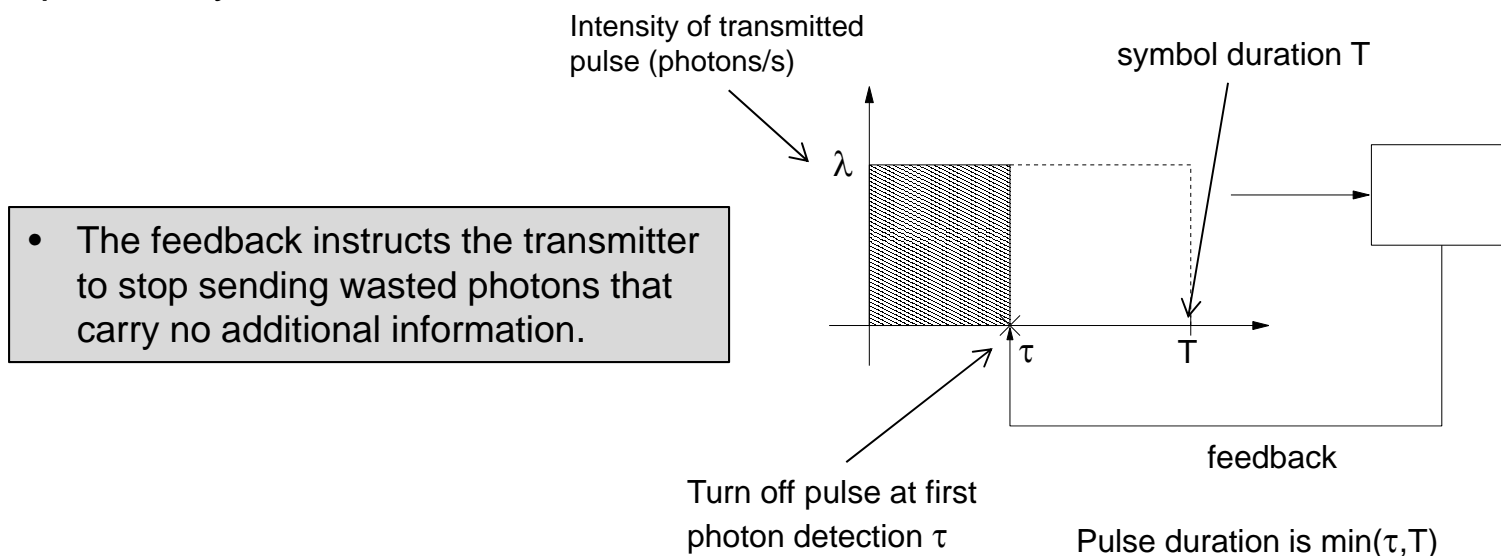


For single-photon number states, the deviation from Holevo capacity is by a constant factor for a given channel, i.e., for a given transmissivity η .



Approximating number-state communication using coherent states with single-photon shutoff

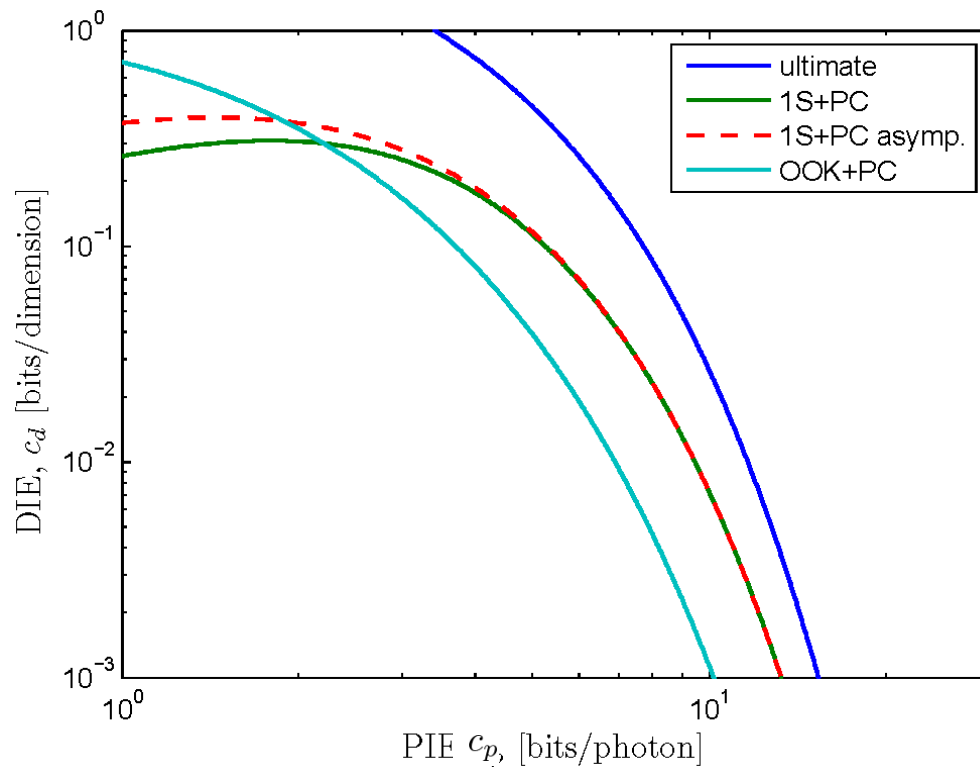
- We can *mimic* the ideal photodetection statistics of the single-photon number state using *receiver-to-transmitter feedback*:
 - The transmitter uses standard OOK or PPM modulation, and starts sending a coherent-state pulse every time the modulator calls for an “ON” signal.
 - A standard photon-counting receiver is used.
 - Utilizing (ideal, instantaneous, costfree — i.e., **very impractical**) feedback from the receiver, the transmitter turns off its pulse as soon as the first photon is detected.
 - If the transmitted pulse has very high intensity (“**photon blasting**”), this will ensure that at least one (and therefore exactly one) photon will be detected, with very high probability.



Asymptotic capacity of coherent states with single-photon shutoff

- Coherent-state OOK with single-photon shutoff economizes on photons by a factor $d(\epsilon)$, but expands bandwidth usage by the same factor $d(\epsilon)$, where ϵ is the pulse detection probability.
- This tradeoff is favorable at high PIE (and disadvantageous at high DIE).
- The asymptotic capacity efficiency tradeoff is:

$$c_d^{1S}(c_p) \approx (e c_p 2^{-c_p}) \max_{\epsilon \in [0,1]} \left[\frac{2^{-h_2(\epsilon)}}{d(\epsilon)} \right]$$



achieved at optimal value:

$$\epsilon^* \approx 0.88$$

$$d(\epsilon^*) \approx 2.38$$

$$\lambda T \approx 2.1 \text{ photons}$$

$$\bar{n} \approx 0.876p$$

Summary of some Holevo capacity-approaching schemes

Table below shows the *asymptotic ratio*, at high PIE, of DIE for the specified scheme to the optimal Holevo DIE at the same PIE.

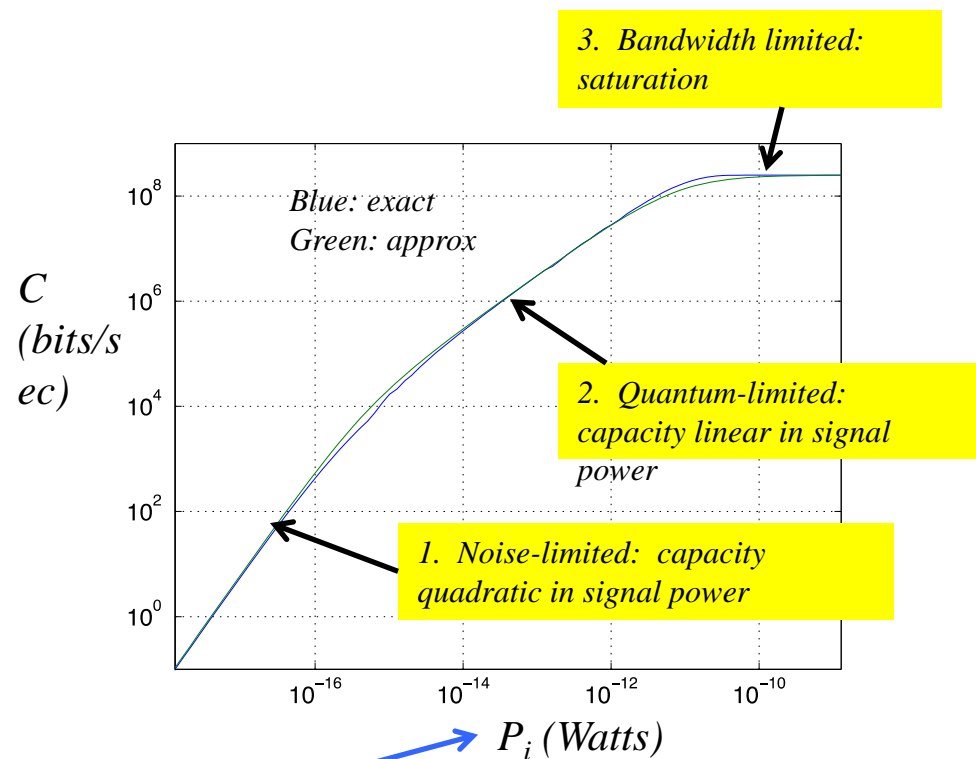
- ϵ is the non-erasure probability (detection probability) for the coherent state cases.
- η is the end-to-end efficiency for the number state cases.

	Coherent states with single-photon shutoff		Single-photon number states		
	general ϵ	@ opt. ϵ^*	general η	@ equiv. $\eta_{\text{eq}}(\epsilon^*)$	@ opt. η^*
OOK	$\frac{2^{-h_2(\epsilon)}}{d(\epsilon)}$	0.274 @ $\epsilon^* = 0.876$	$2^{-h_2(\eta)}$	0.274 @ $\eta_{\text{eq}} = 0.534$	1.000 @ $\eta^* = 1$
PPM	$\frac{\epsilon/e}{d(\epsilon)}$	0.150 @ $\epsilon^* = 0.715$	η/e	0.150 @ $\eta_{\text{eq}} = 0.407$	0.368 @ $\eta^* = 1$



Poisson model for PPM channel capacity with noise

- A Poisson channel model is used for detection of signal in background noise.
- The Poisson PPM channel capacity does not, in general, have a closed form solution.
- Approximations exist that provide insight into its behavior.
- The IM-PC channel has three regions as a function of the signal power:
 1. Noise-limited: capacity is quadratic in signal power.
 2. Quantum-limited: capacity is linear in signal power.
 3. Band-width limited: capacity saturates.
- This differs from the coherent channel which is linear or bandwidth limited.



P_i = minimum required power to close the link

- Determined by inverting the **capacity function** at the target data rate.
- All other system components (receiver, decoder, detector, etc.) are assumed to be **ideal** (no losses).

$$C \approx \frac{1}{\ln(2)E_\lambda} \left(\frac{P_i^2}{P_i \frac{1}{\ln(M)} + P_n \frac{2}{M-1} + P_i^2 \frac{MT_s}{\ln(M)E_\lambda}} \right) \text{ bits/sec}$$

2.
1.
3.

P_n = noise power

M = PPM order

E_λ = energy per photon

T_s = slot width



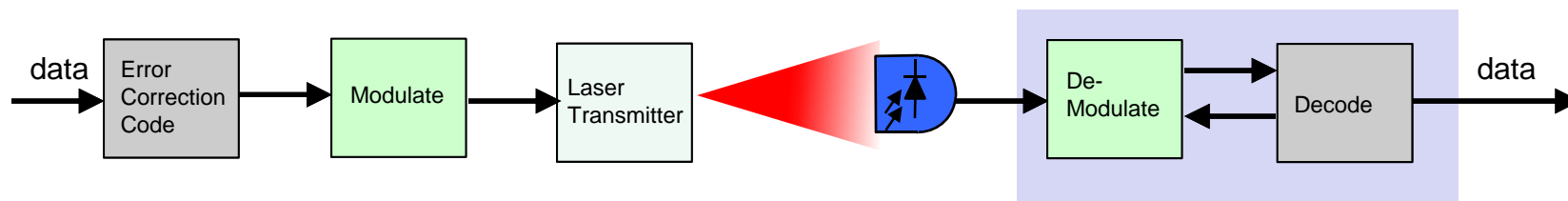
Coding to approach capacity

In this section, we discuss:

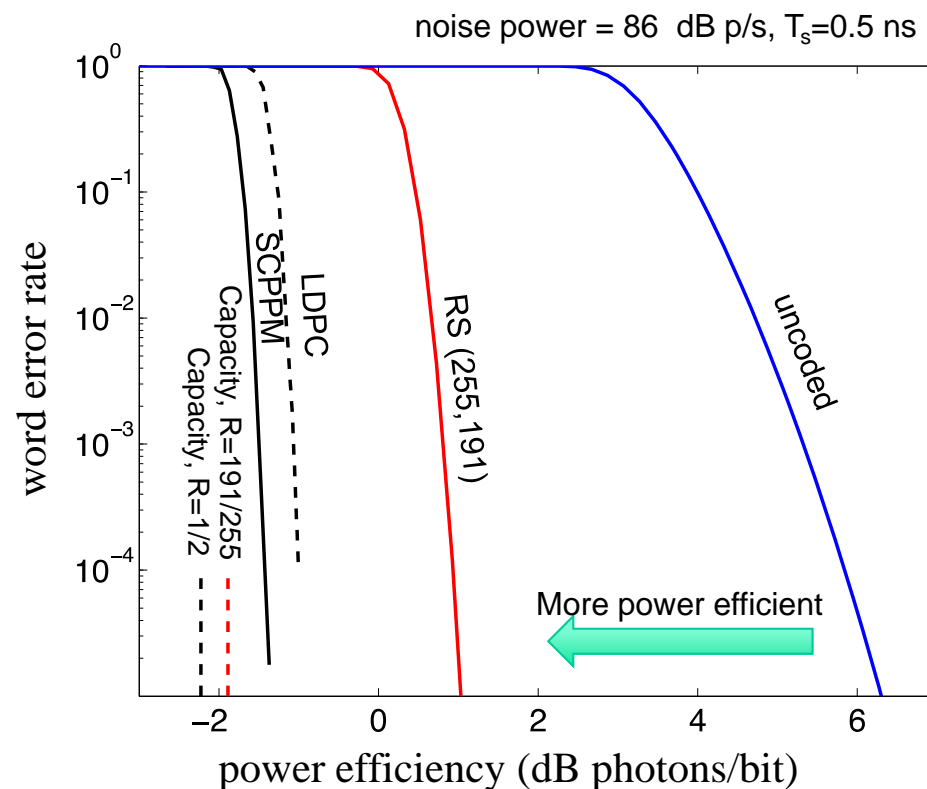
- **Choice of error correction code**
- **Code inefficiency relative to capacity limit**



Approaching capacity with an error correction code



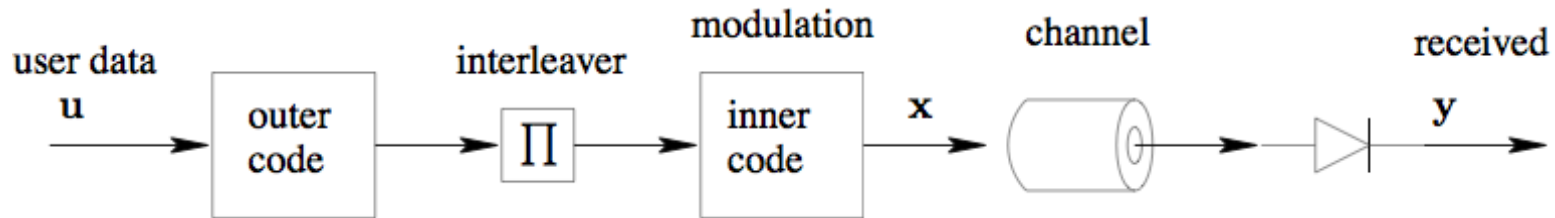
- We signal utilizing a very power efficient error-correction code (ECC) that performs close to the capacity limit.
- With high probability, a codeword error will result if the signal power drops below the channel capacity.
- Pulse-Position-Modulation (PPM) contains memory, and may be considered part of the ECC.
- Iterative demodulation and decoding (of properly designed codes) provides gains of ~ 1.5 dB over non-iterative decoding.
- Codes designed explicitly for use with PPM provide gains over more general-purpose codes.





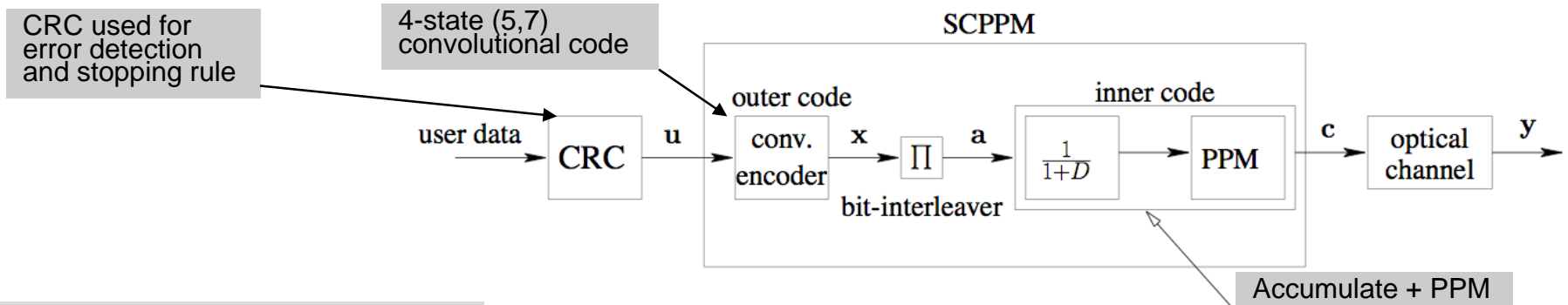
Some possible choices of code

Goal: Choose a code type that has near-capacity performance over all operating points, and low encoding/decoding complexity.



	outer code(s)	inner code
<i>hard decisions</i> →	RSPPM Reed-Solomon $(n,k)=(M^a-1)$, $a=1$ [McEliece, 81], $a>1$ [Hamkins, Moision, 03]	PPM
<i>soft decisions</i> →	PCPPM parallel concatenated convolutional [Kiasaleh, 98], [Hamkins, 99] (DTMRF, iterate with PPM [Peleg, Shamaï, 00])	PPM
	SCPPM convolutional [Massey, 81] (iterate with APPM) [Hamkins, Moision, 02]	(accumulate) PPM
	LDPC-PPM low density parity check [Barsoum, 05]	PPM

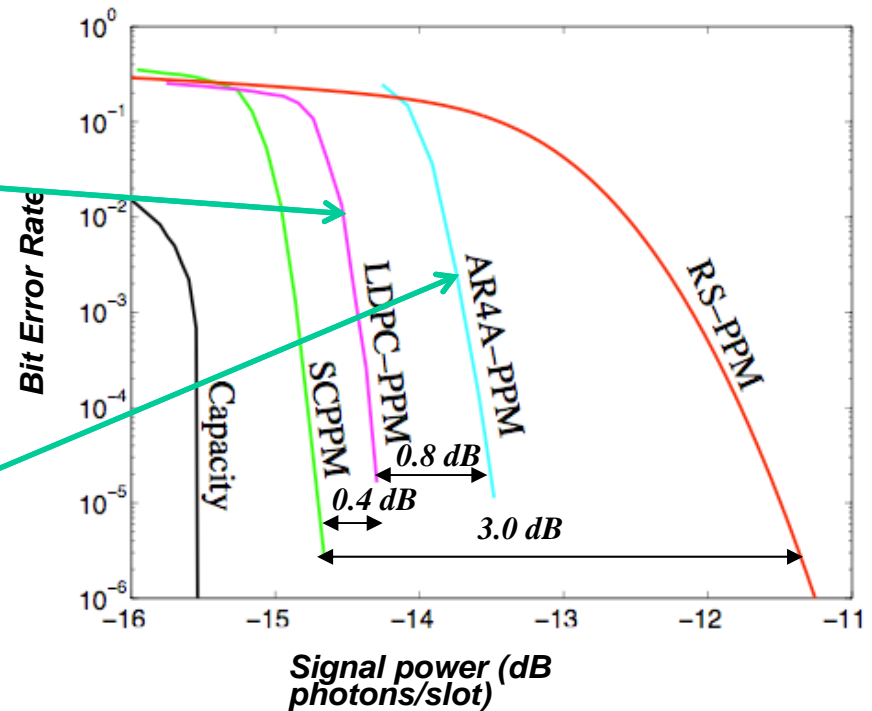
Example of SCPPM code architecture



- The most power efficient class of codes known for the noisy Poisson PPM channel are the serial concatenation of convolutional code with an accumulator and PPM (SCPPM)
- 3.3 -- 1.8 dB gain over baseline Reed-Solomon coded PPM ($R=1/2$)
- 0.4 dB gain over best known LDPC-coded PPM
- Complexity, performance favors SCPPM over LDPC-coded PPM

LDPC code designed for PPM channel

LDPC code designed for BPSK channel



Operating point: ($n_b=0.2$ photons/slot, $M=64$, $T_s=32$ nsec)

Loss due to code inefficiency with respect to capacity



$$P_{rqd} = P_i / L_b L_j L_f L_t \eta_{det} \eta_{imp} \eta_{code} \eta_{int}$$

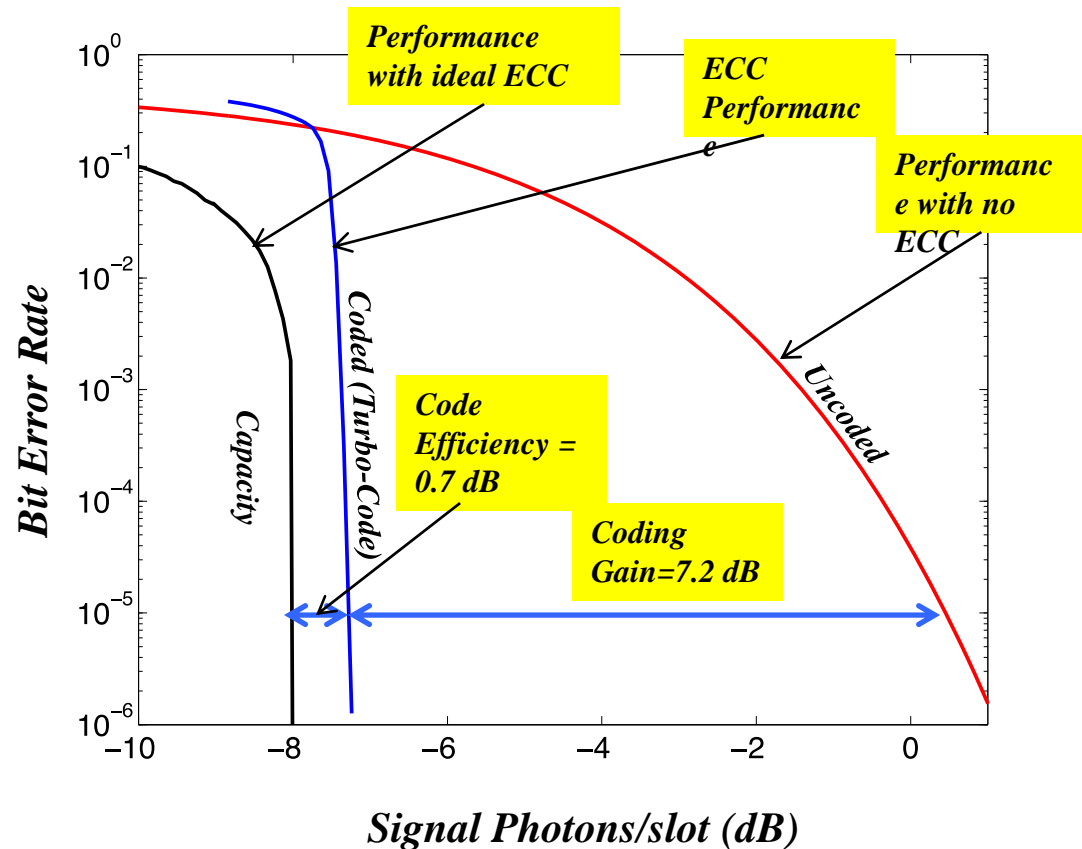
- Measures of the error-control-code (ECC) performance:

1. Coding Gain = (code threshold) – (uncoded threshold)

2. Code Efficiency = (capacity threshold) – (code threshold)

- We use **code efficiency** η_{code} to measure ECC performance:

- Provides an immediate measure of additional gain that is possible by changing the code.
- For modern codes (LDPC, turbo), code efficiency is well characterized as constant over varying conditions, while error-rates do not have closed-form solutions.





Poisson-modeled noises

In this section, we discuss capacity limits with:

- Thermal noise
- Finite laser transmitter extinction ratio
- Dark noise at the detector

Fundamental limit on capacity efficiency in noise

Classical (Shannon Capacity)

Channel described by input/output alphabets and probability map from input to output

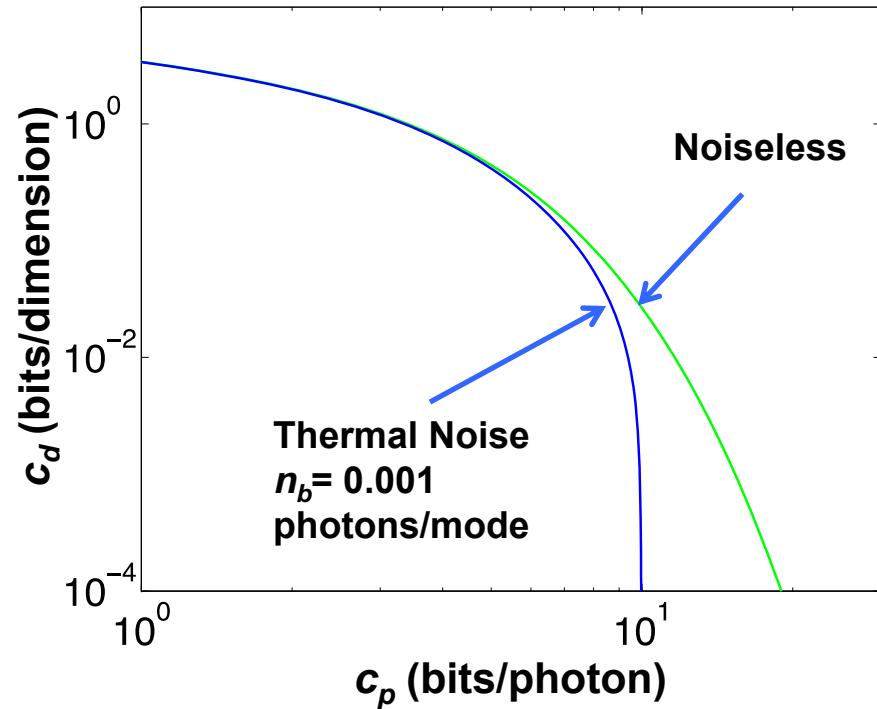
Quantum (Holevo Capacity)

Optimize Shannon capacity over all possible measurements (select probability map)

Characterize Efficiency:

c_p = bits/photon (e.g., (bits/s)/Watt)

c_d = bits/dimension (e.g., (bits/s)/Hz)



$$g(x) = (1 + x) \log_2(1 + x) - x \log_2(x)$$

Noiseless

$$c_d^{\text{Hol}}(n_b) = g(\bar{n}_s) \quad (\text{bits/dim})$$

$$c_p^{\text{Hol}} = c_d^{\text{Hol}} \bar{n}_s \quad (\text{bits/photon})$$

Thermal Noise (conjectured)

$$c_d^{\text{Hol}}(n_b) = g(\bar{n}_s + \bar{n}_b) - g(\bar{n}_b) \quad (\text{bits/dim})$$

$$c_p^{\text{Hol}}(n_b) = c_d^{\text{Hol}}(n_b) \bar{n}_s \quad (\text{bits/photon})$$

Noisy Poisson OOK channel for thermal noise

- K background noise modes (white, Gaussian), N counts/mode

$$p_1(k; K) = \frac{N^k}{(1+N)^{k+K}} L_k^{(K-1)} \left(\frac{-n_s}{N(1+N)} \right) e^{-n_s/(1+N)} \quad \text{Negative binomial}$$

$$p_1(n; K) \xrightarrow{K \rightarrow \infty} \frac{(n_b + n_s)^n e^{-(n_b + n_s)}}{n!} \quad (n_b = KN) \quad \text{Poisson}$$

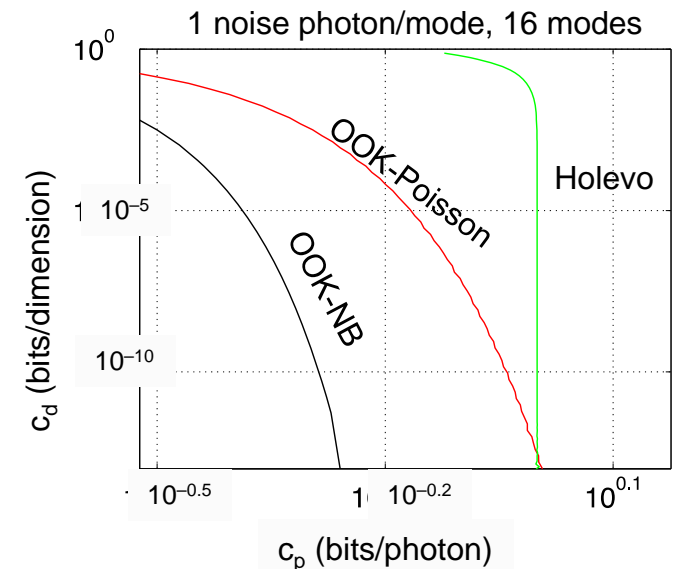
- Photon information efficiency of Poisson OOK channel is unbounded

$$c_p^{\text{OOK}} \geq \left(\left(1 + \frac{n_b}{n_s} \right) \log_2 \left(1 + \frac{n_s}{n_b} \right) - \frac{1}{\ln 2} - \frac{1}{n_s} \right) \xrightarrow{n_s \rightarrow \infty} \infty$$

- Holevo limit (conjectured) is bounded

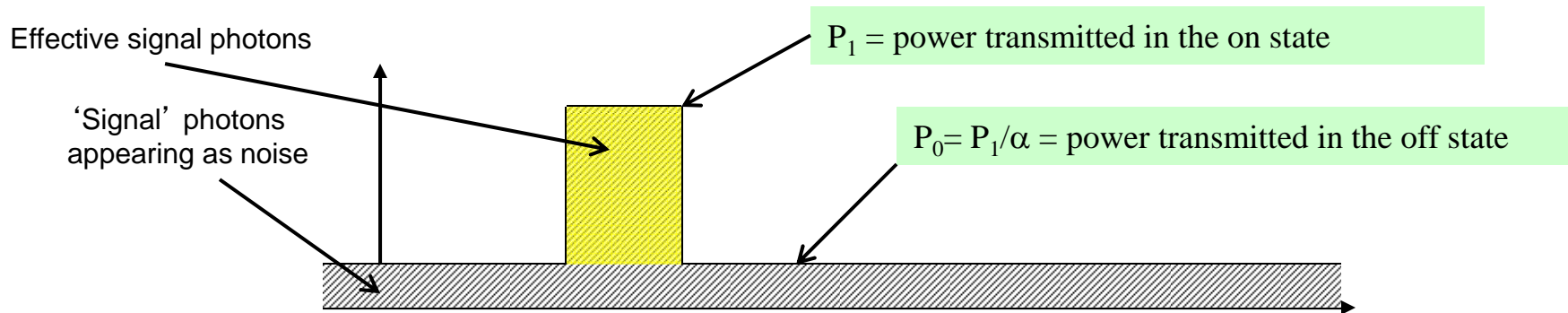
$$c_p^{\text{Hol}}(n_b) \leq \log_2(1 + 1/n_b)$$

➔ **Poisson approximation to multimode thermal noise must become inaccurate at large c_p for any number of noise modes.**



Noisy Poisson OOK channel for finite laser extinction ratio

- Non-ideal transmitters transmit some power in the “OFF” state:
 - Power transmitted in the “OFF” state is **proportional** to power in the “ON” state; the proportionality constant is the **extinction ratio α** .



- Finite transmitter extinction ratio generates a Poisson-distributed **background noise proportional to the signal**, $n_b = n_s/\alpha$.
- With finite extinction ratio α , the photon efficiency of OOK + photon counting is strictly bounded:

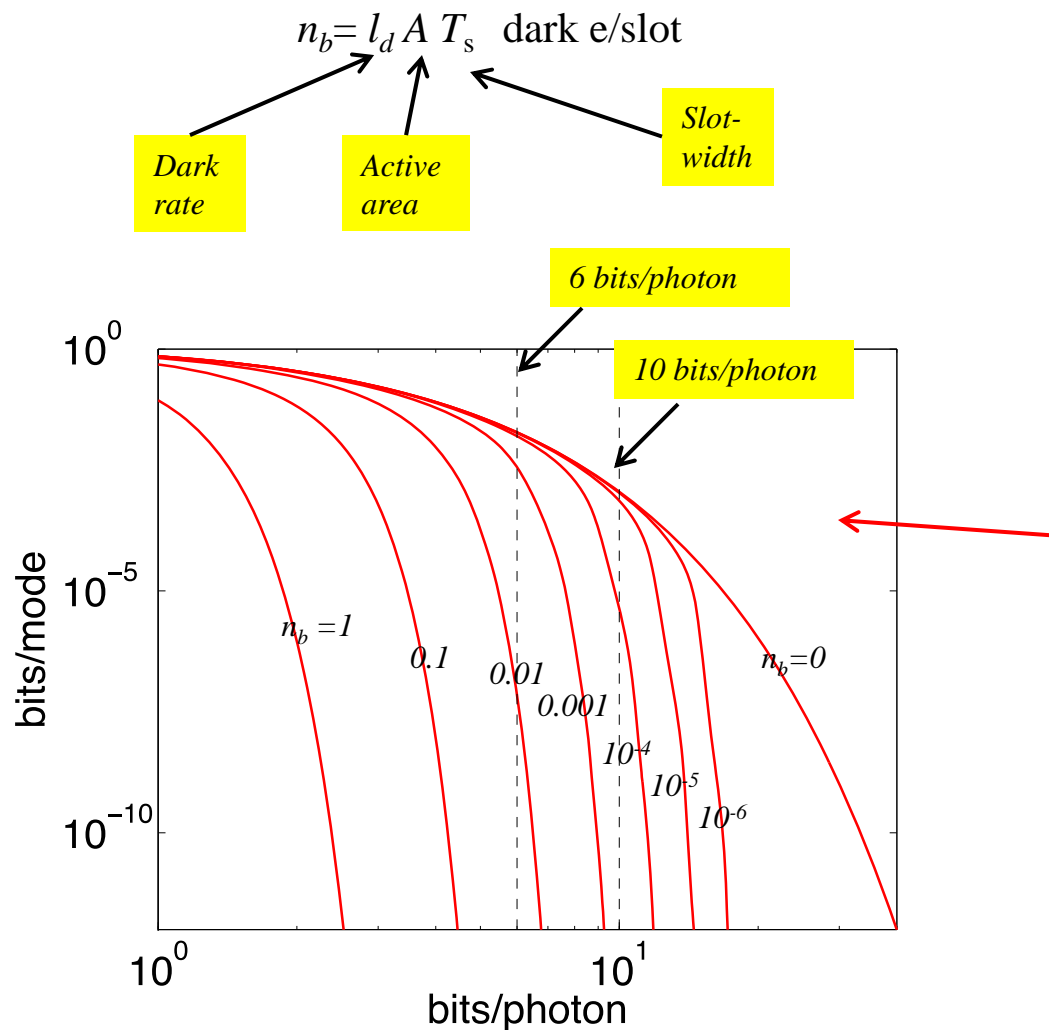
$$c_p \lesssim \log_2(\alpha) - 1/\ln(2) \text{ (bits/effective signal photon)}$$



Dark noise at the photodetector

- Photodetectors produce **dark noise**, which are spurious photo-electrons that are present even with no incident light.

- Dark current generates a Poisson-distributed **signal-independent background noise** n_b .



Device	I_d (e/s/mm ²)
Si GM-APD	10^6
InGaAsP GM-APD	10^8
NbN SNSPD	10^2

- Noise levels with $n_b > 10^{-5}$ incur large losses at 10 bits/photon.
- Mitigation, by decreasing A and T_s , has limits
 - A can only be decreased to the diffraction limit.
 - T_s can only be decreased to bandwidth limit, and we will show that decreasing T_s also exacerbates other losses.

Noisy Poisson OOK channel for detector dark noise

- With nonzero dark rate n_b , the photon efficiency of OOK + photon counting is technically unbounded, but is **effectively bounded**, because c_d drops off **doubly-exponentially** in a noisy Poisson channel.
 - c_d is approximately upper bounded by $c_d < \beta c_p 2^{-\beta c_p}$ where $\beta = \max(1, en_b 2^{c_p})$
 - See the nearly vertical aqua curve, below its intersection with the noiseless Holevo bound (where $\beta > 1$).
 - This approximate bound crosses the noiseless OOK and Holevo curves at

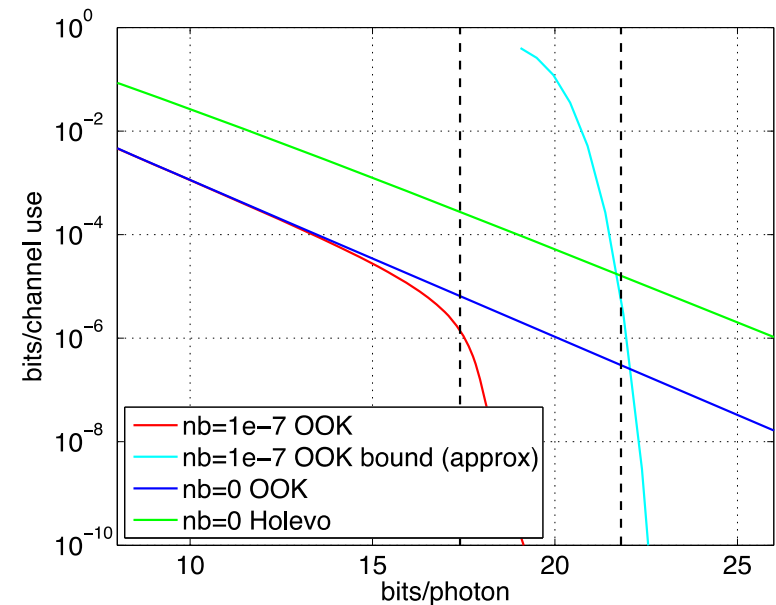
$$c_p \approx \log_2 \left(\frac{1}{en_b} \right)$$

- The actual c_d breaks away sharply from the noiseless OOK curve starting at a lower value of c_p , estimated empirically to be:

$$c_p \approx \log_2 \left(\frac{1}{e^4 n_b} \right) \Big|_{n_b=10^{-7}} = 17.4 \text{ bits/photon}$$

- This breakaway point can also be interpreted as:

$$M n_b \approx 1/e^4 = 0.018 \text{ noise counts/PPM symbol}$$

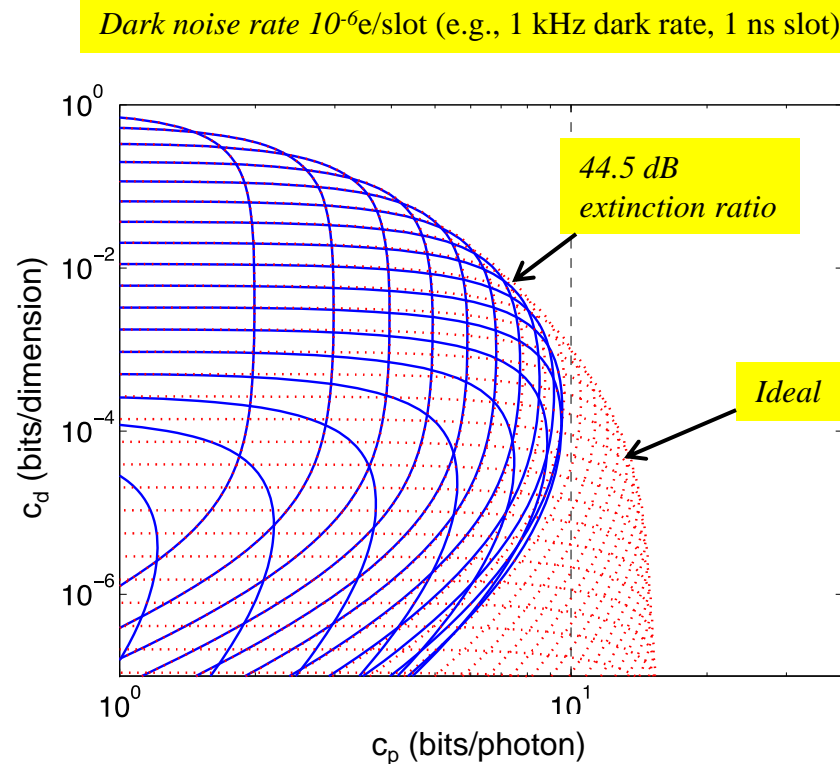
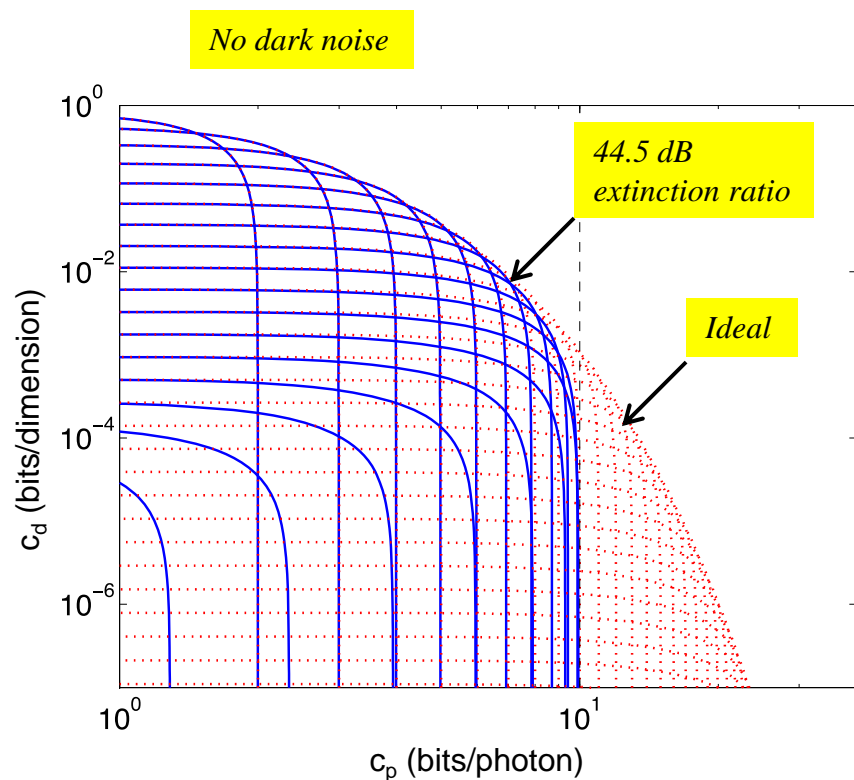


Thus, achieving **arbitrarily high** c_p on the noisy Poisson channel becomes impractical.



Capacity limits with dark noise & finite extinction ratio

- Each curve in these plots is the capacity efficiency tradeoff for a given PPM order M , and is generated by varying the average number of signal photons.





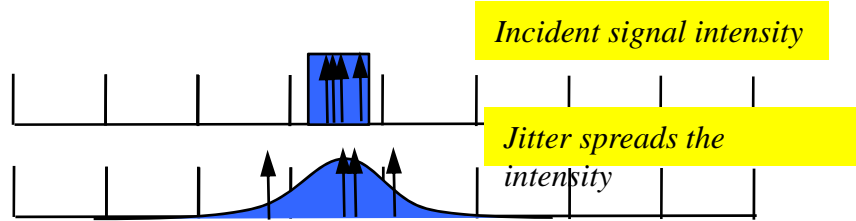
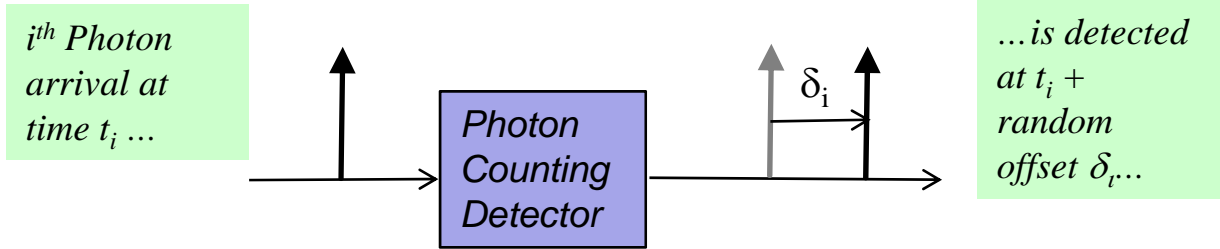
Other losses at the detector

In this section, we discuss:

- **Detector jitter**
- **Photodetector blocking**
- **Overall system engineering**



Detector jitter



- Jitter is the **random delay** from the time a photon is incident on a photo-detector to the time a photo-electron is detected.
- Jitter losses are a function of the **normalized jitter standard deviation**:

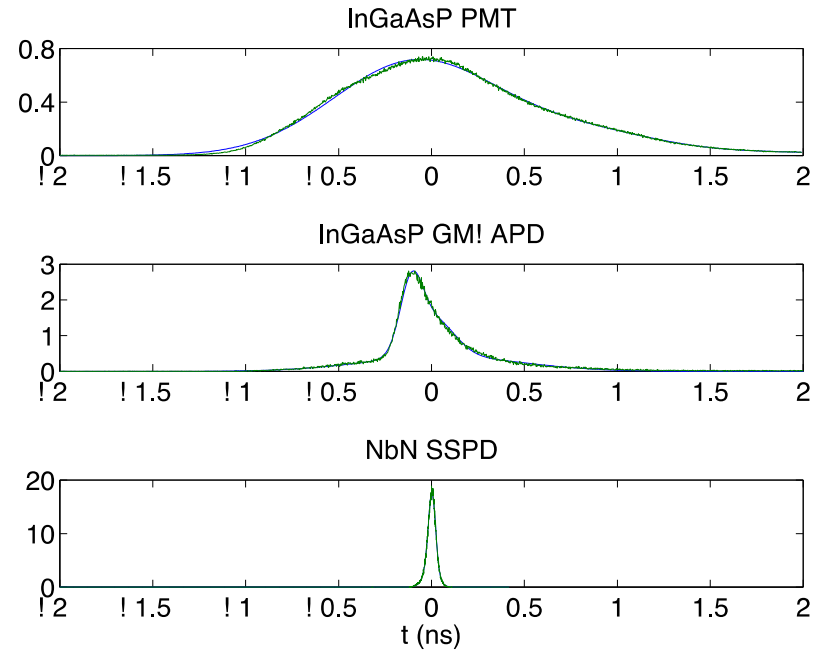
$$\frac{\sigma_j}{T_s}$$

← jitter standard deviation

← Slot-width

- Thus, jitter limits our ability to decrease the slot width T_s without incurring loss.

Measured jitter densities for some candidate detectors

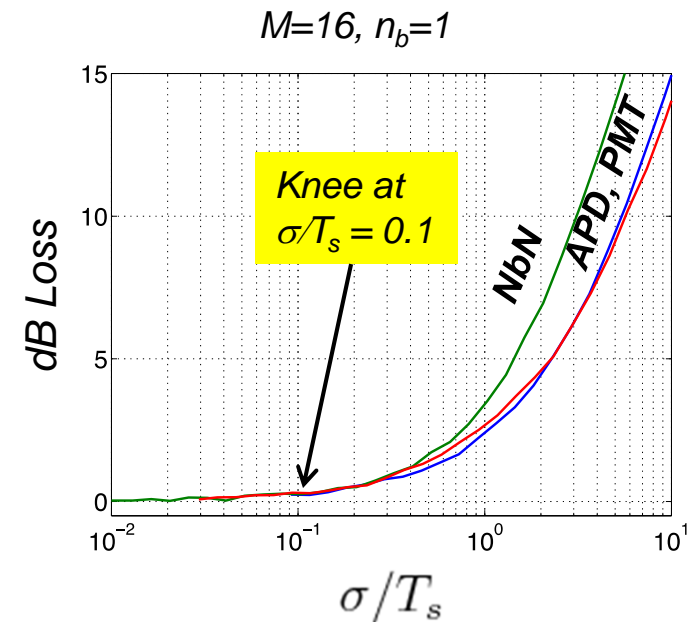
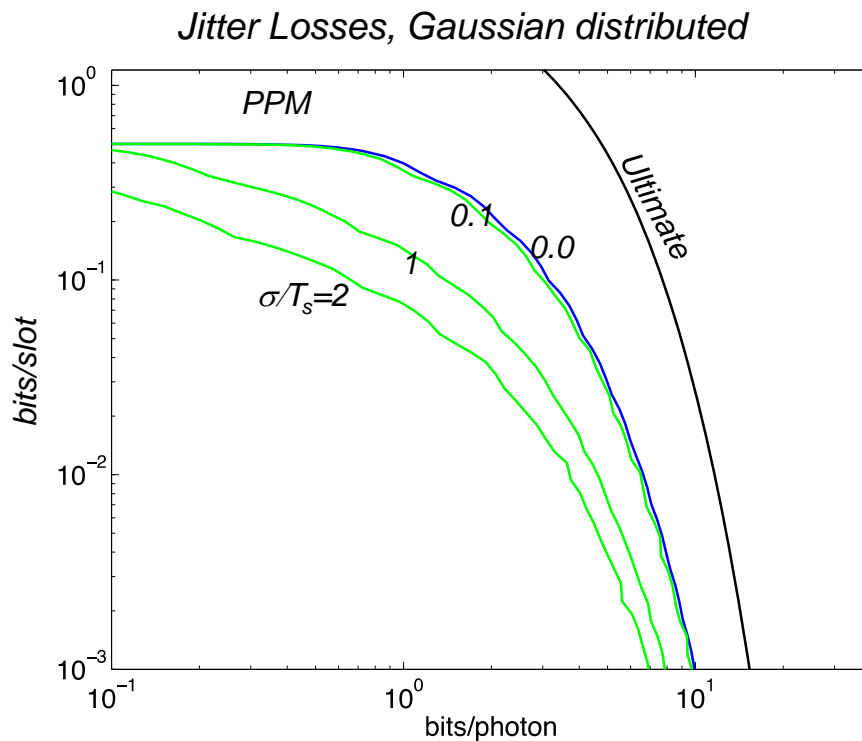




Losses due to detector jitter

$$P_{rqd} = P_i / L_b L_j L_f L_t \eta_{det} \eta_{imp} \eta_{code} \eta_{int}$$

- Significant losses for $\sigma/T_s > 0.1$
- Effectively enforces a lower bound on T_s
 - Limits data rate
 - Limits ability to mitigate dark noise



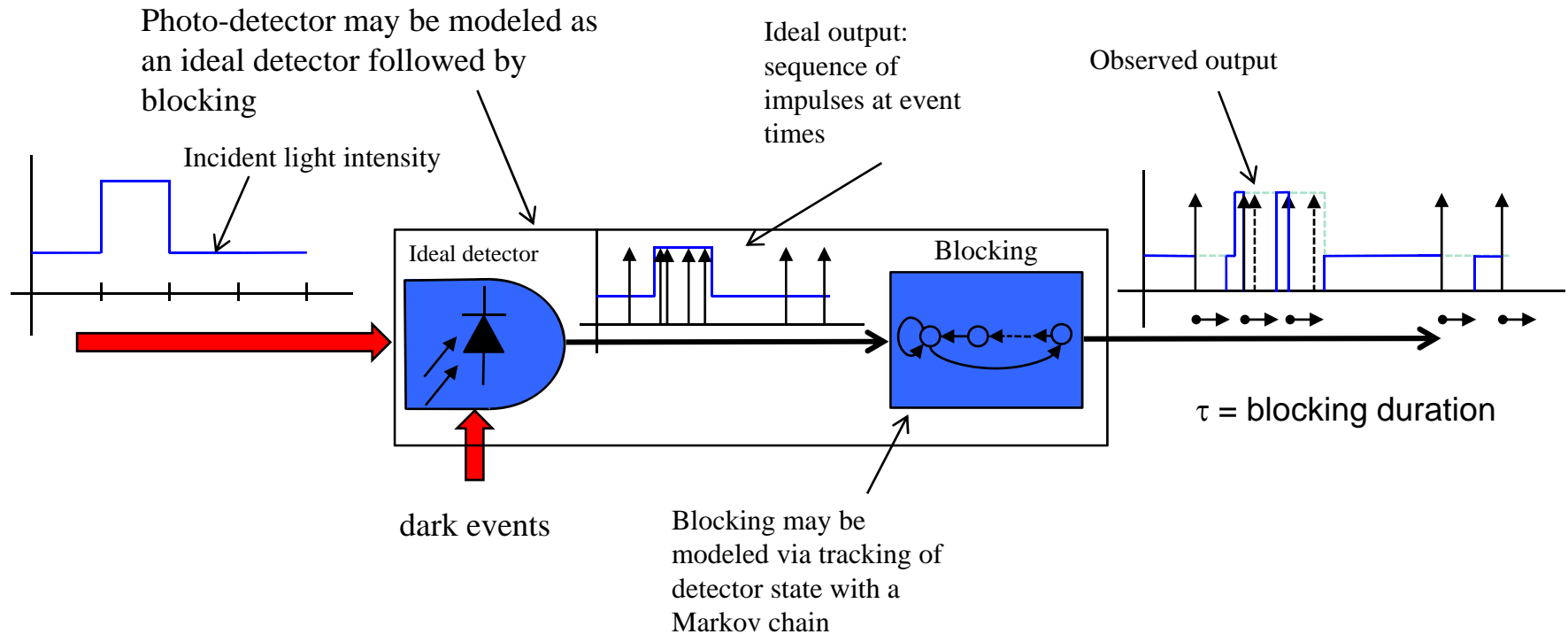
Device	σ / ns
InGaAs(P) PMT	0.9
InGaAs(P) GM-APD	0.3
Si GM-APD	0.24
NbN SNSPD	0.03

Photodetector blocking

$$P_{rqd} = P_i / L_b L_j L_f L_t \eta_{det} \eta_{imp} \eta_{code} \eta_{int}$$

- Certain photon-counting photodetectors are rendered inoperative (**blocked**) for some time τ (**dead time**) after each detection event
 - 10–50 ns, Si GM-APD
 - 1–10 μ s, InGaAs GM-APD
 - 3–20 ns, NbN SNSPD

Characterize impact of blocking by $\mu =$ probability detector is unblocked





Mitigating blocking

Blocking may be mitigated by decreasing the peak incident photon rate (per detector)

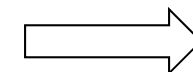
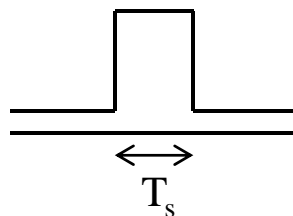
$\mu = \text{probability}$
detector is unblocked

$$\mu \approx \frac{1}{1 + \tau l}$$

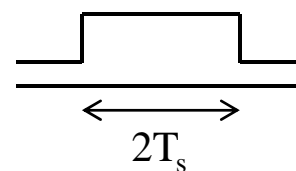
dead-time: fixed by the device

photon rate: decreased by temporal or spatial diffusion

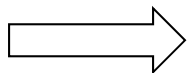
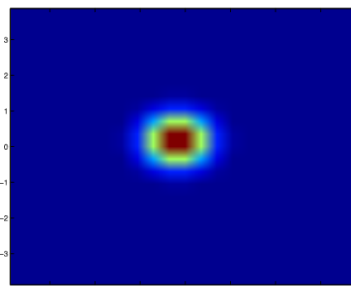
- Temporally
 - Increase the slot-width and reduce the photon rate, while preserving the photons/slot.
 - Reduces impact of blocking, but lowers the data rate (bits/s), and integrates more noise



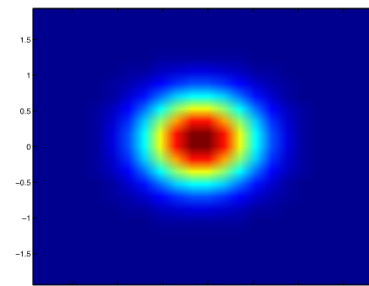
Make signal more diffuse in time



- Spatially
 - Increase Focal length, to decrease signal intensity in the focal (detector) plane
 - Integrates more noise



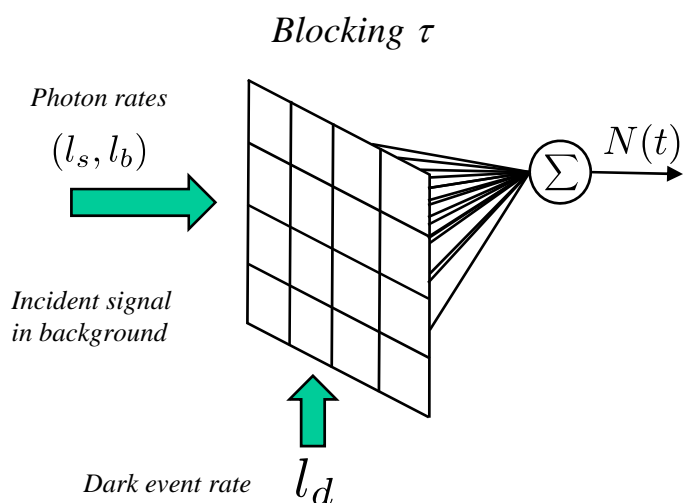
Make signal more diffuse in space



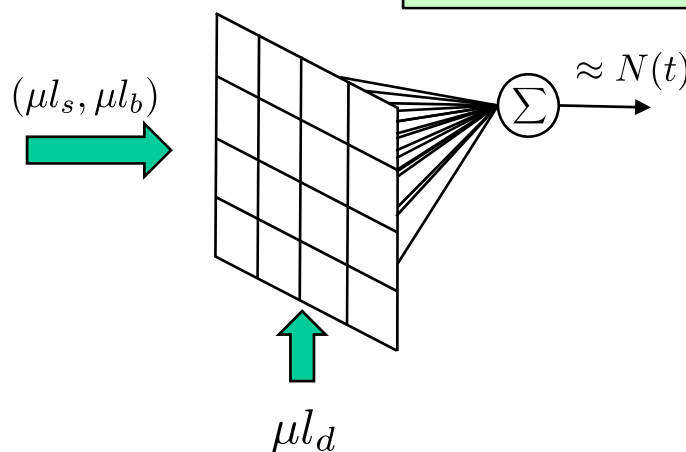
We investigated this approach, numerically determining the optimum F number for a given blocking, dark noise, and target data rate (which fixes the aggregate required signal flux)



Modeling blocking loss with arrayed detectors

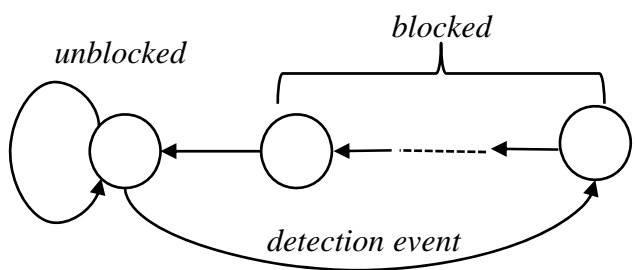


Approximate Model ($\tau = 0$)



Array output may be approximated as Poisson. Blocking attenuates the signal and noise.

Markov Model of Detector State



$\mu = \text{probability detector is unblocked}$

$$\mu \approx \frac{1}{1 + \tau l} \quad l = \text{incident photon rate}$$

Signal Power Loss:
increase in power to achieve fixed capacity

$$C_b(l'_s) = C_u(l_s)$$

$$\frac{l_s}{l'_s} \approx \begin{cases} \mu & \text{high SNR} \\ \sqrt{\mu} & \text{low SNR} \end{cases}$$

Capacity Loss:
decrease in capacity at fixed signal power

$$\begin{array}{l} \text{blocked capacity} \longrightarrow \\ \text{unblocked capacity} \longrightarrow \end{array} \frac{C_b}{C_u} = \mu$$



Overall system engineering considerations

- Mitigation of impairments results in conflicting demands on resources, hence requiring system engineering to optimize.

Parameter	Blocking	Jitter	Dark Noise
F/D			
T_s			
M			



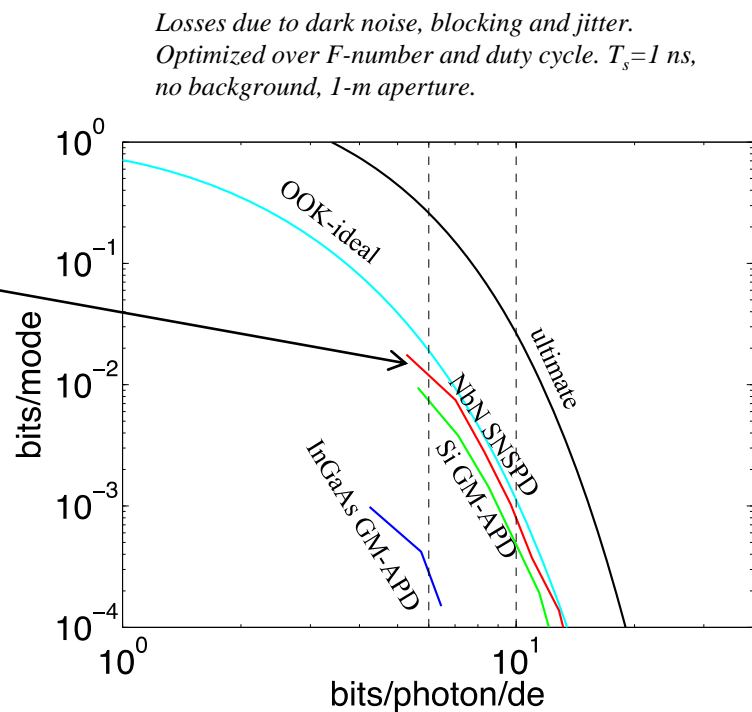
Mitigated by decreasing this parameter



Mitigated by increasing this parameter

Device requirements for high bits/photon operation

Non-ideality	Requirement	NbN SNSPD, $T_s=1$ ns
Extinction Ratio	$\alpha > 60$ dB	(presumed infinite for graph)
Jitter	$\sigma/T_s < 0.1$	0.03
Dark Noise	$I_d T_s < 10^{-5}$	10^{-9}
Blocking	$I_p \tau \ll 1.0$	10^{-4}





Atmospheric effects on optical communication

In this section, we discuss:

- **The effects of:**
 - **Background radiation**
 - **Absorption/scattering**
 - **Clear sky turbulence effects**
 - **Pointing errors**
- **Fading channel models**
- **Mitigating the effects of fading**

Atmospheric effects on optical communication



- **Background Radiation**
- **Absorption/Scattering**
- **Clear Sky Turbulence Effects**
 - **Scintillation**
 - **Angle-of-Arrival Variations**
 - **Beam Spread**
 - **Beam Wander**

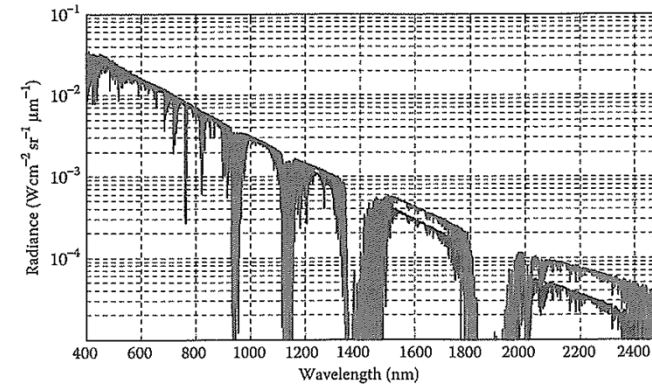
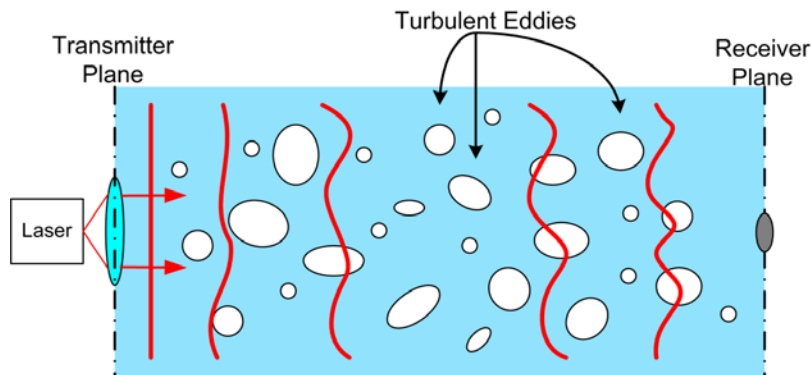


FIGURE 8.16 Daytime sky radiance at 2 km above sea level. The Sun zenith angle is 45°. Two cases (radiance curves) are shown: (1) the observer zenith angle on the ground is at 40° (higher radiance curve) and (2) the observer zenith angle on the ground is at 70° (lower radiance curve). The rural aerosol model with a visibility of 23 km at sea level was used. Data obtained after MODTRAN simulation.

[Piazzolla, '09]



264

Near-Earth Laser Communications

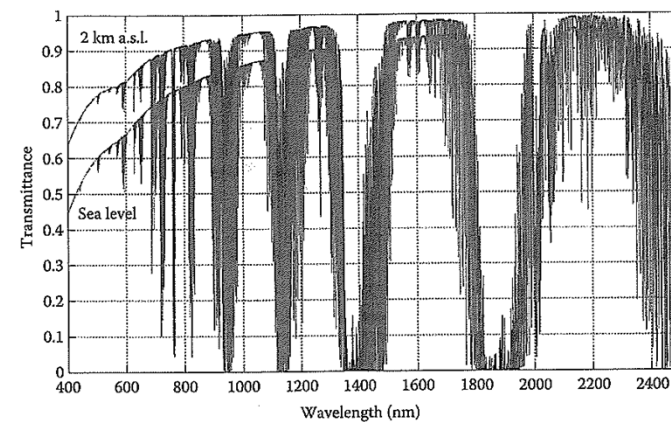


FIGURE 8.12 Atmospheric transmittance in an Earth-to-space path at zenith. A rural aerosol composition with a surface visual range of 23 km is considered. The data refers to the case of an observer located at two elevations: sea level (lower transmittance) and 2 km above sea level.



Background Scattered Light

$$P_{rqd} = P_i / L_b L_j L_f L_t \eta_{det} \eta_{imp} \eta_{code} \eta_{int}$$

- Aperture open to atmosphere also collects background light (scattered sunlight, light from point sources)
- Background light degrades performance

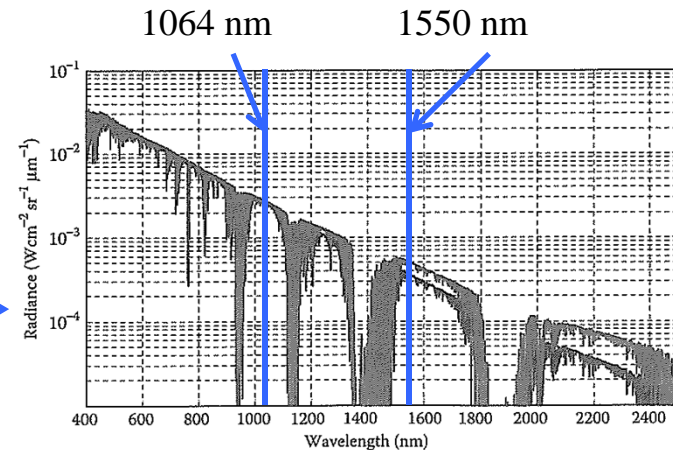
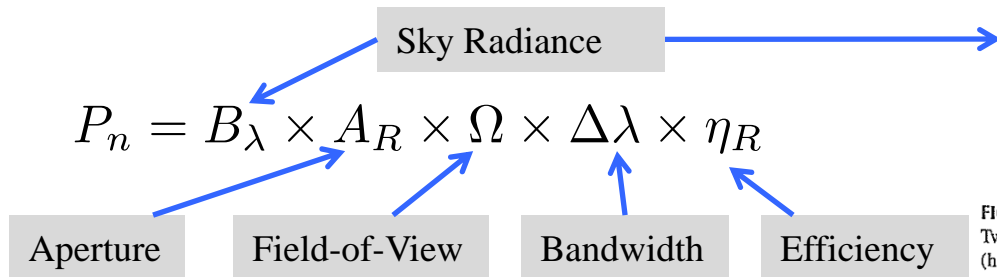
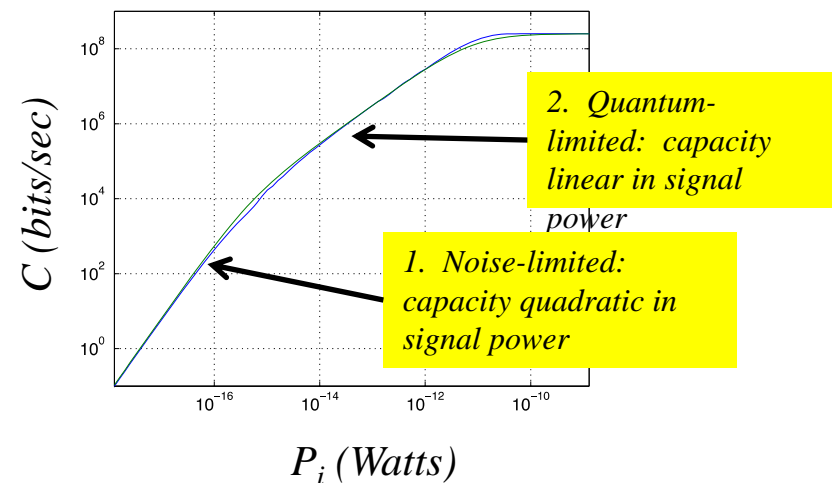


FIGURE 8.16 Daytime sky radiance at 2km above sea level. The Sun zenith angle is 45°. Two cases (radiance curves) are shown: (1) the observer zenith angle on the ground is at 40° (higher radiance curve) and (2) the observer zenith angle on the ground is at 70° (lower radiance curve). The rural aerosol model with a visibility of 23 km at sea level was used. Data obtained after MODTRAN simulation.

- Impact of noise depends on the signal to noise ratio, and modulation
- Must be taken into account for choice of wavelength
- At large background noise, coherent detection becomes favorable

$$C \approx \frac{1}{\ln(2)E_\lambda} \left(\frac{P_i^2}{P_i \frac{1}{\ln(M)} + P_n \frac{2}{M-1} + P_i^2 \frac{MT_s}{\ln(M)E_\lambda}} \right) \text{ bits/sec}$$

[Piazzolla, '09]





Absorption/Scattering

$$P_{rx} = P_t G_t G_r L_s L_a \eta_{pt} \eta_t \eta_r$$

- Absorption and Scattering from aerosols (dust, etc.) and molecules (water vapor, etc.) attenuate the signal
- In bad weather (rain, snow, fog), attenuation can be severe, causing dropouts
- In Clear Sky, must budget for attenuation
- Drives selection of bands with good clear sky transmissivity
 - Candidates for Earth-Space link: 1064, 1550 nm
- Typical attenuation for Space-Earth link in near-infrared at zenith 0.1—0.3 dB
- Outages at low elevation angles

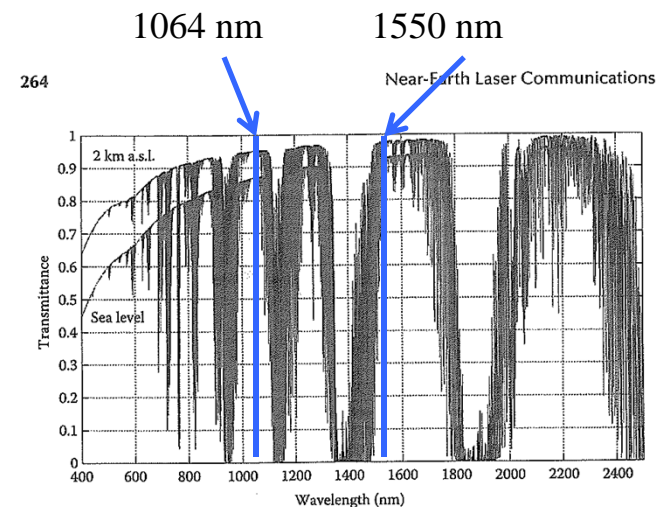


FIGURE 8.12 Atmospheric transmittance in an Earth-to-space path at zenith. A rural aerosol composition with a surface visual range of 23 km is considered. The data refers to the case of an observer located at two elevations: sea level (lower transmittance) and 2 km above sea level.

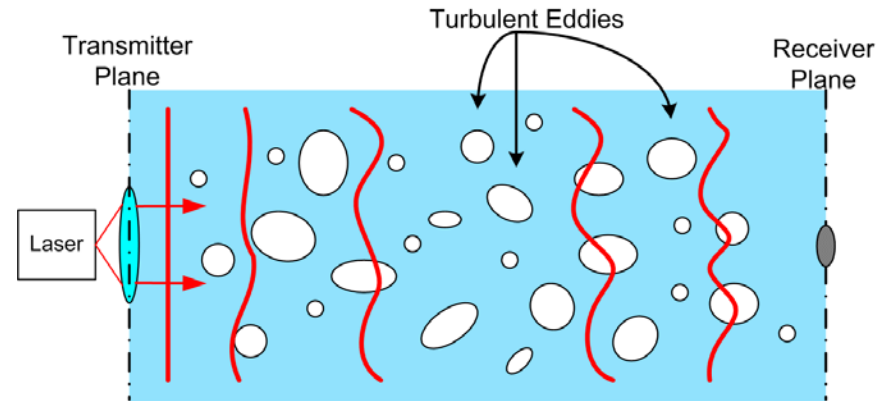
[Piazzolla, '09]



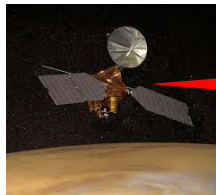
Clear Sky Turbulence

- **Random spatio-temporal mixing of air with different temperatures causes refractive-index variations**

- **Scintillation**
(constructive/destructive interference)
- **Angle-of-arrival variations**
- **Beam spreading**
- **Beam wander**



- **Asymmetric Impacts:**



Space-to-Earth:
Angle-of-arrival
(spatial distortion)
Scintillation (fading)



Earth-to-Space:
Beam spread
(attenuation)
Beam wander (fading)

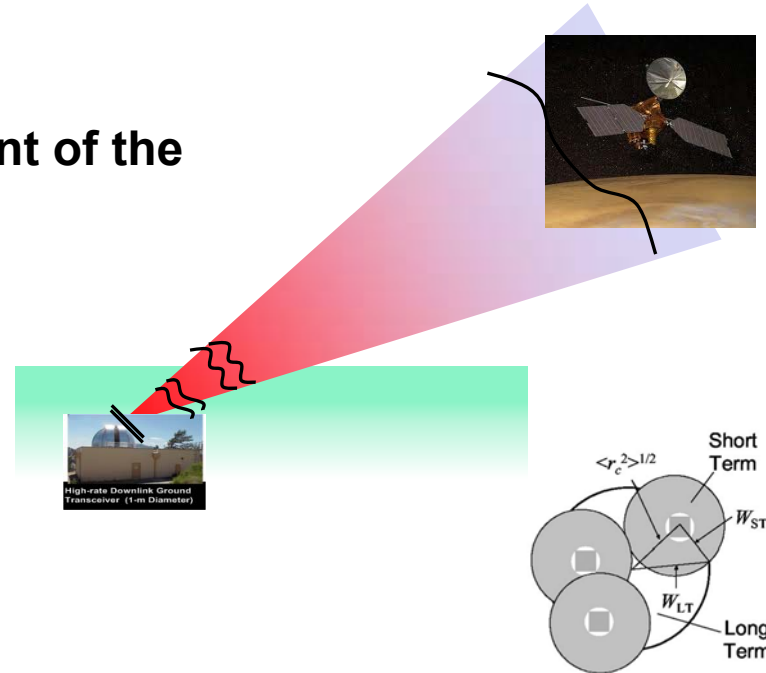
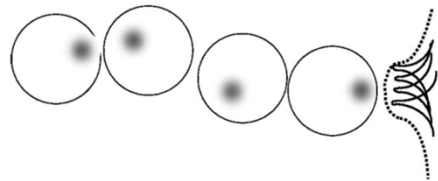
Atmosphere (mostly concentrated in 0-20 km)



Beam Wander (Scintillation) & Beam Spread (Attenuation)



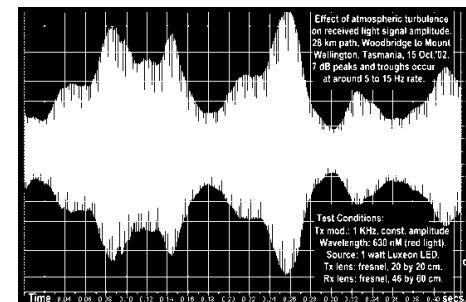
- Turbulence is a thin phase-screen in front of the transmitter aperture
- Coherence length is up to meters
 - Receiver always sees *plane wave*
 - Focused beam is diffraction-limited
 - Diffraction-limited spot moves in focal plane



- Beam-spread (attenuation)
 - Linear phase at transmitter *tilts* the beam
 - Higher-order phase *spreads* the beam (short-exposure < 1 msec)

Andrews & Phillips, Opt. Eng. (2006)

- Beam-Wander → Scintillation
 - Irradiance fluctuates with log-normal distribution
 - Multiple transmit beams used to reduce scintillation

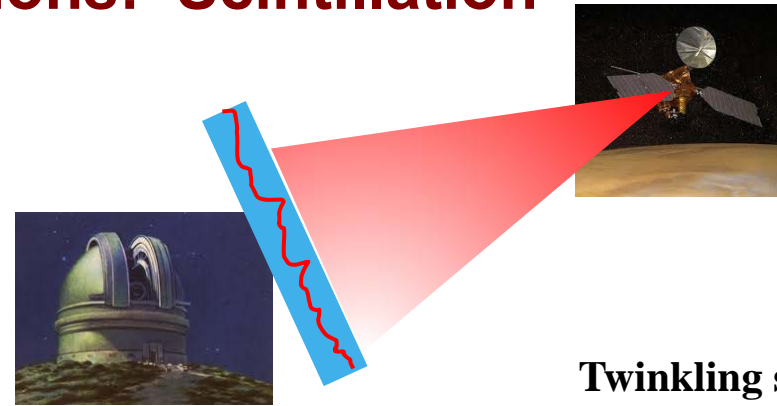


<http://www.modulatedlight.org>

Temporal Distortions: Scintillation



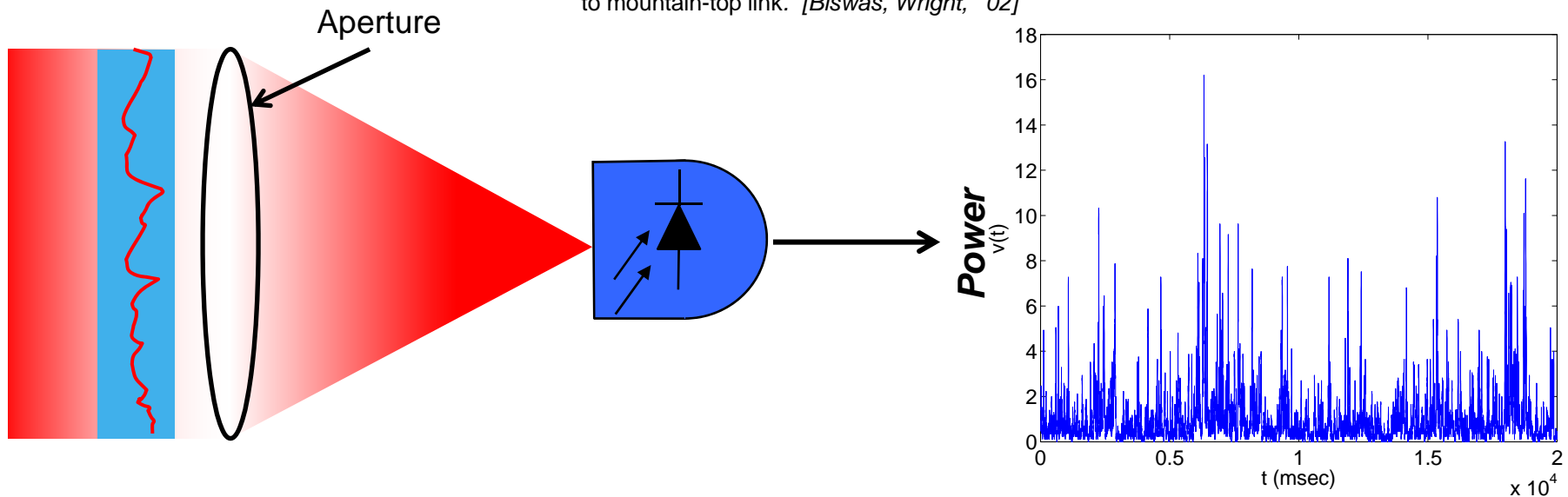
- Random refractive index fluctuations also lead to phase distortions—constructive and destructive interference.
- Leads to Scintillation, random power fluctuations
- Each “coherence cell” has independent amplitude
 - Aperture averaging: averaging over multiple coherence cells reduces the fluctuation in power (law of large numbers)



Twinkling stars

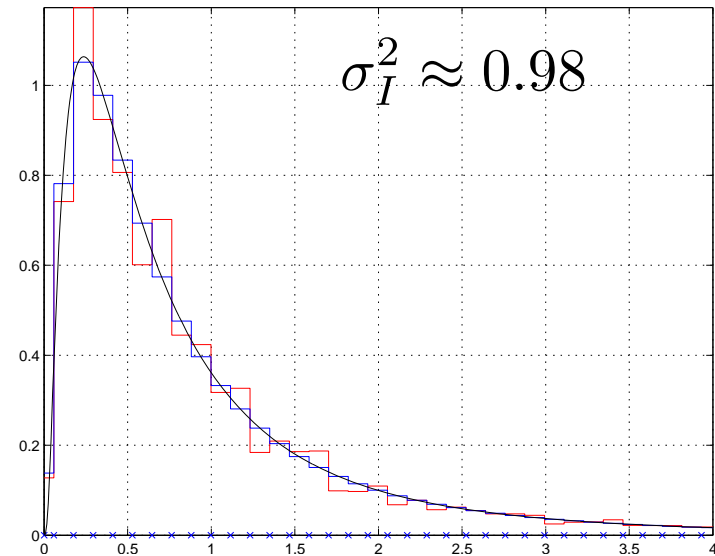
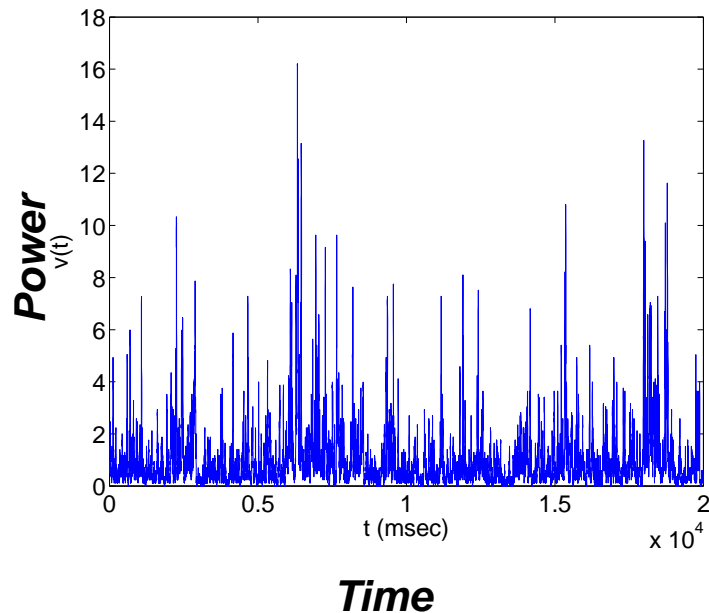


Measured fluctuations over a 45-km mountain-top to mountain-top link. [Biswas, Wright, '02]





Modeling scintillation: scintillation index



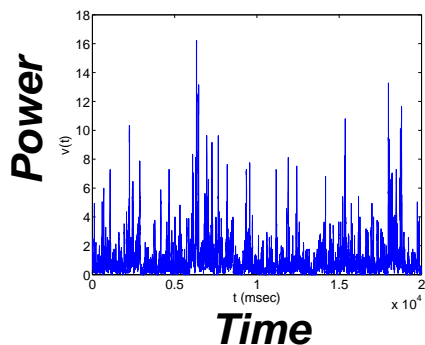
Random instantaneous power fluctuation in weak turbulence is well-modeled as log-normally distributed

$\sigma_I^2 =$ scintillation index

$$f_V(v) = \frac{1}{\sqrt{2\pi\sigma_I^2}} \frac{1}{v} \exp\left(\frac{-(\log v + \sigma_I^2/2)^2}{2\sigma_I^2}\right)$$

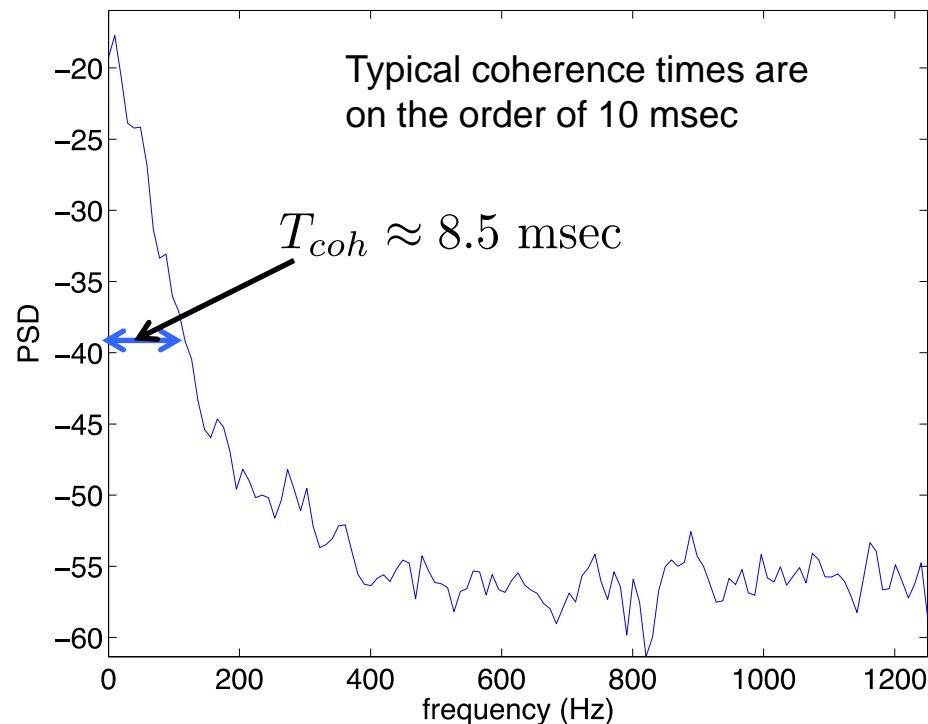


Modeling scintillation: coherence time



The power is highly correlated over short time intervals. The coherence time is the minimum duration over which two samples are (approximately) uncorrelated.

Coherence time goes as 1/band-width. 90% bandwidth is commonly used.



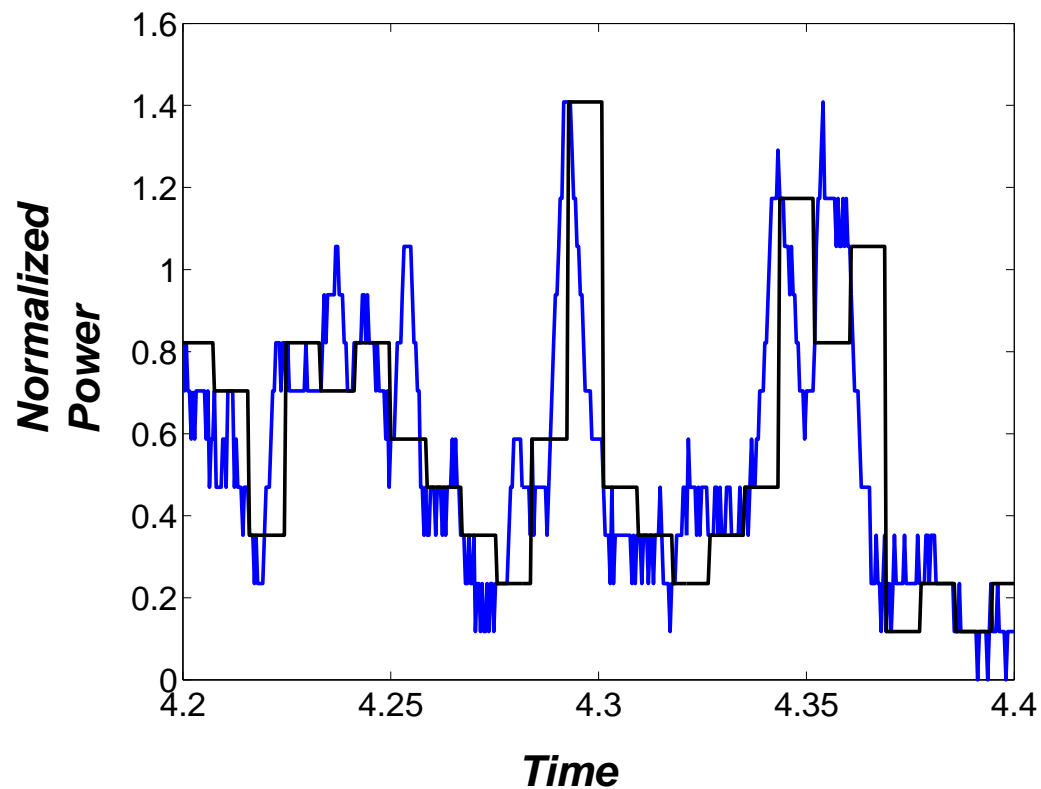
T_{coh} = coherence time

$$W(\xi) = \min \left\{ 2B \left| \int_{-B}^B S_x(f) df \right| = \xi \int_{-\infty}^{\infty} S_x(f) df \right\}$$

$$T_{coh} = \frac{1}{W(0.90)}$$



Block fading model



Reduce fading to a two-parameter model:

Model fades as drawn independently from a log-normal distribution every T_{coh} seconds, and constant over those intervals.

$$\{\sigma_I^2, T_{coh}\}$$

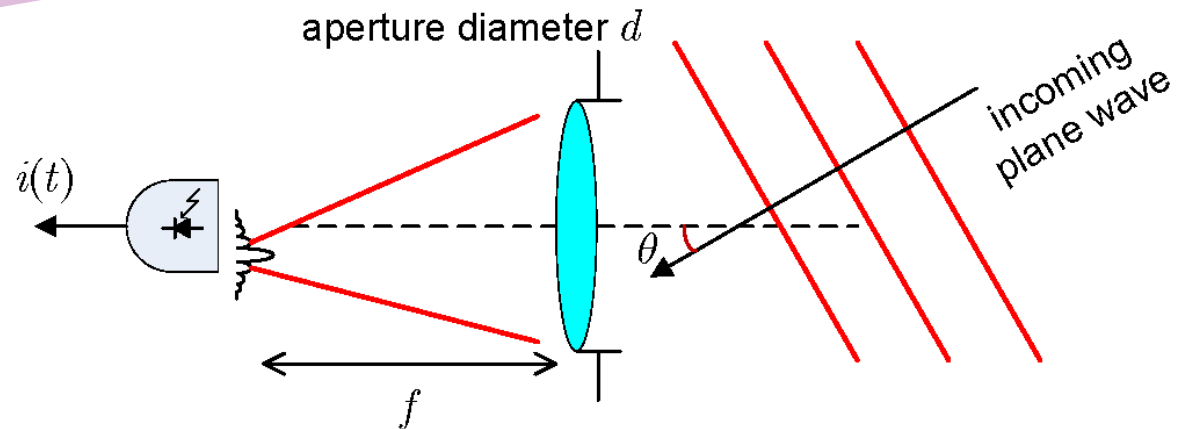
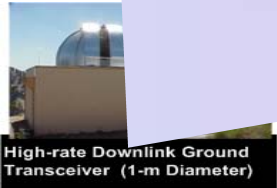
Scintillation Index

Coherence Time

$$T_{coh} \approx 8.5 \text{ msec}$$

$$\sigma_I^2 \approx 0.98$$

Fading due to pointing errors



[Barron, Boroson, '06]

$$L_{\text{static}} \approx 10 \log_{10}(1 + \sigma^2) + 5 \log_{10}(e) \frac{m^2}{1 + \sigma^2} \text{ dB}$$

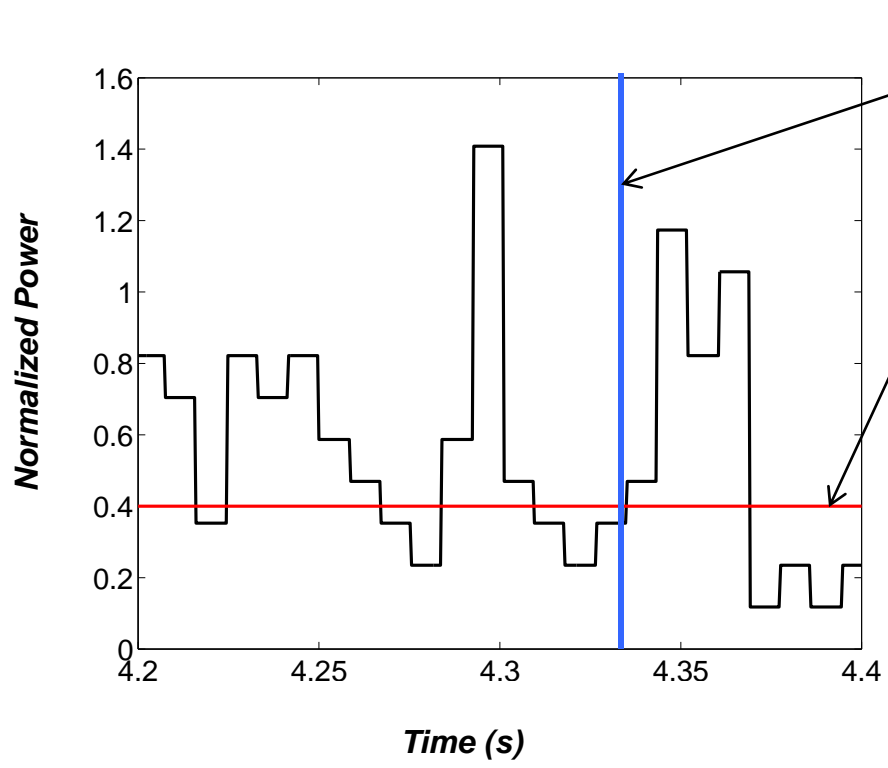
$$L_f \approx 5 \log_{10}(e)(2\sigma^2 + m^2) - L_{\text{static}} \text{ dB}$$

- m=mean pointing error
- σ =pointing error standard deviation
- Gaussian beam, Gaussian pointing errors

Losses due to dynamics similarly are linear in the variance



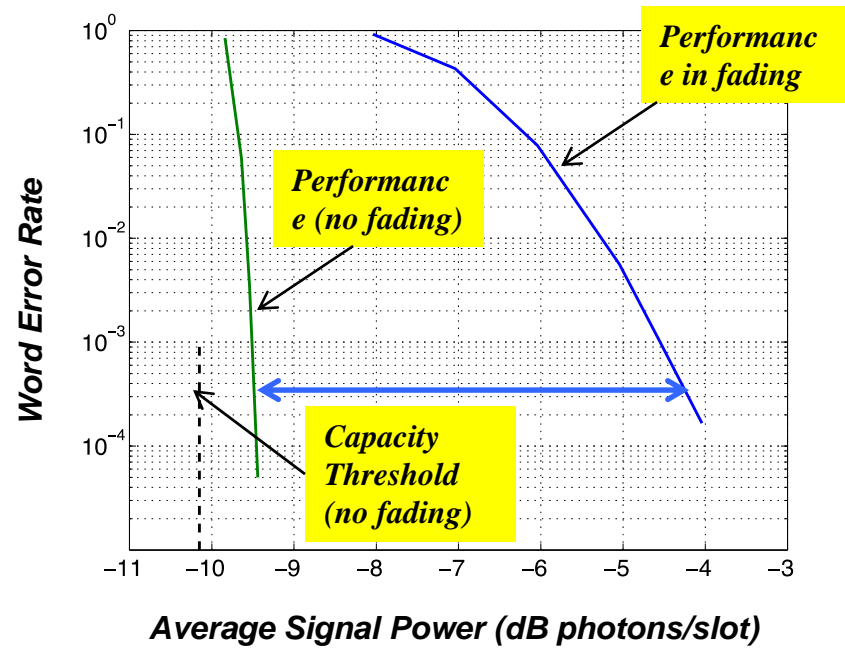
Impact of fading on coded performance: outages



Codeword duration = 0.06 msec (at 125 Mbps data rate) $\ll T_{coh}$

Capacity Threshold

Loss due to outages ~5 dB in this example



Performance in fading

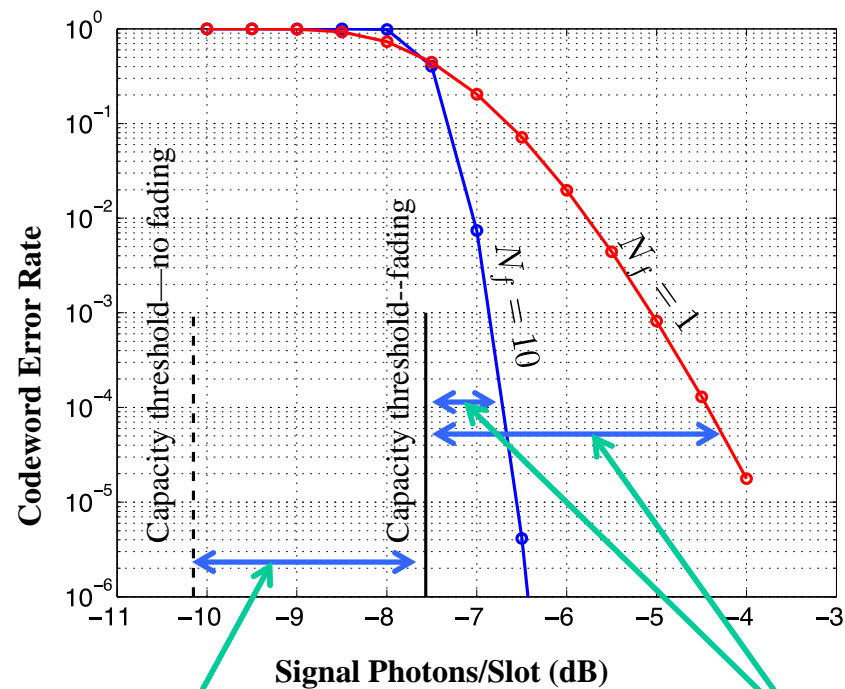
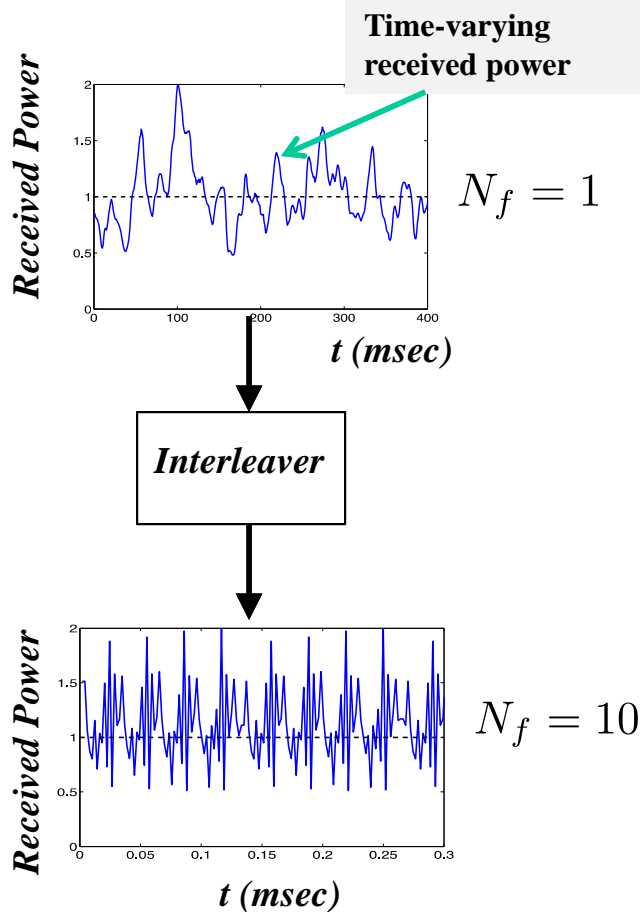
Performance (no fading)

Capacity Threshold (no fading)

Capacity losses due to signal fading

$$P_{rqd} = P_i / L_b L_j L_f L_t \eta_{det} \eta_{imp} \eta_{code} \eta_{int}$$

- N_f = number of uncorrelated fades per codeword
- σ_I^2 = scintillation index (variance of normal in log-normal fading)



Fading capacity loss (unrecoverable)

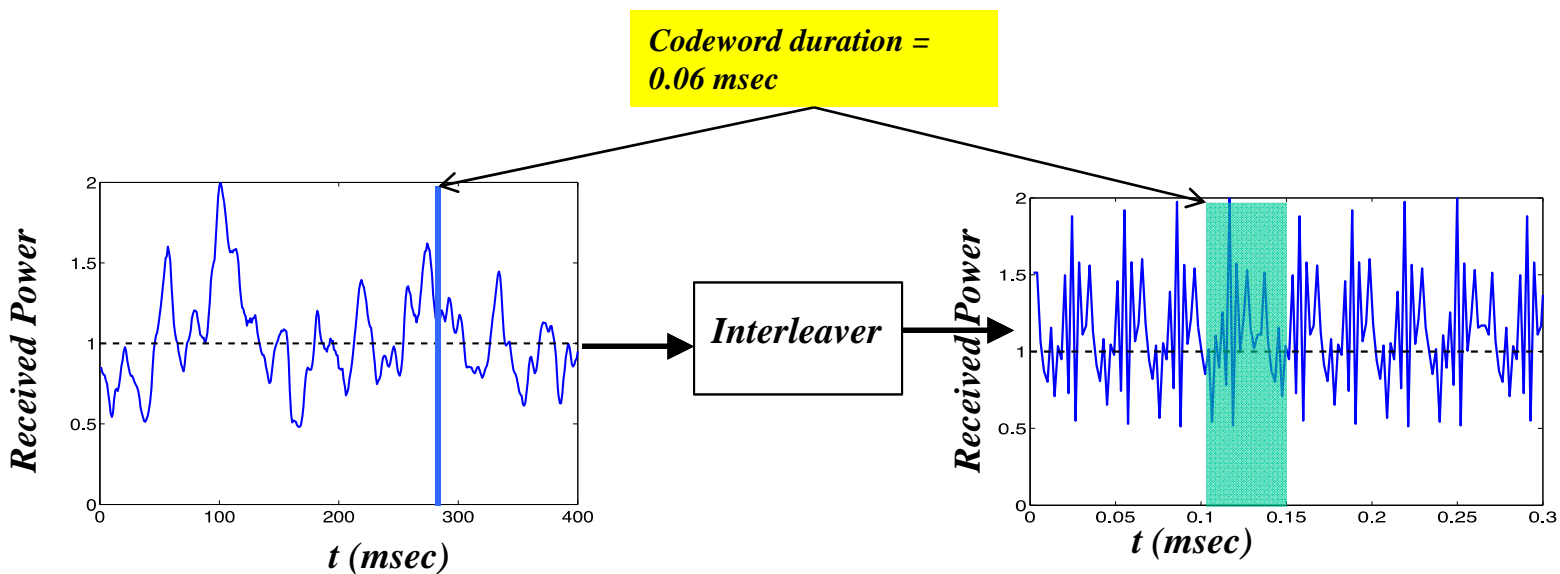
Interleaving Efficiency (mitigated with interleaving)

$$L_f \approx 2.5\sigma_I^2 \text{ dB}$$

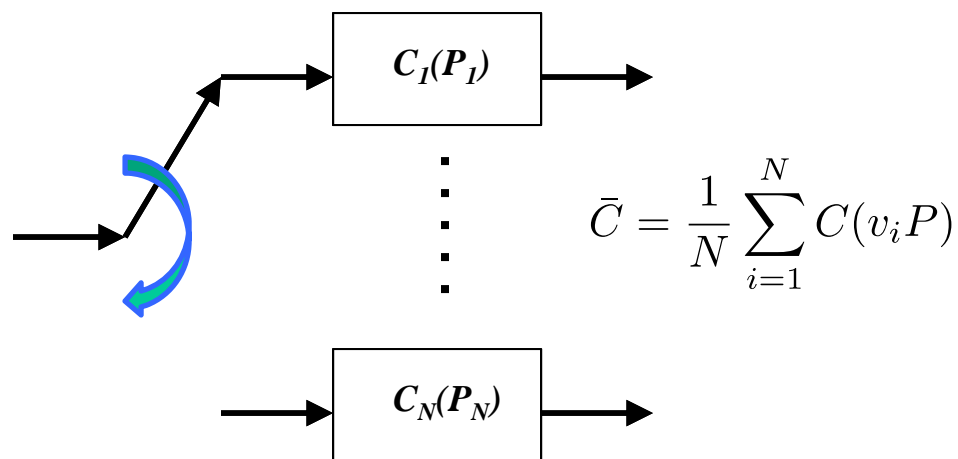
$$\eta_{int} \approx 16 \sqrt{\frac{\sigma_I^2}{N_f}} \text{ dB}$$



Mitigating fading outages with interleaving



- Each codeword now sees N uncorrelated fades, or Powers
- Effectively transmitting over N parallel channels, each with a different power
- Relevant capacity is the *instantaneous capacity*, averaged over the N powers





Interleaving gain and fading capacity

Instantaneous capacity is a random variable

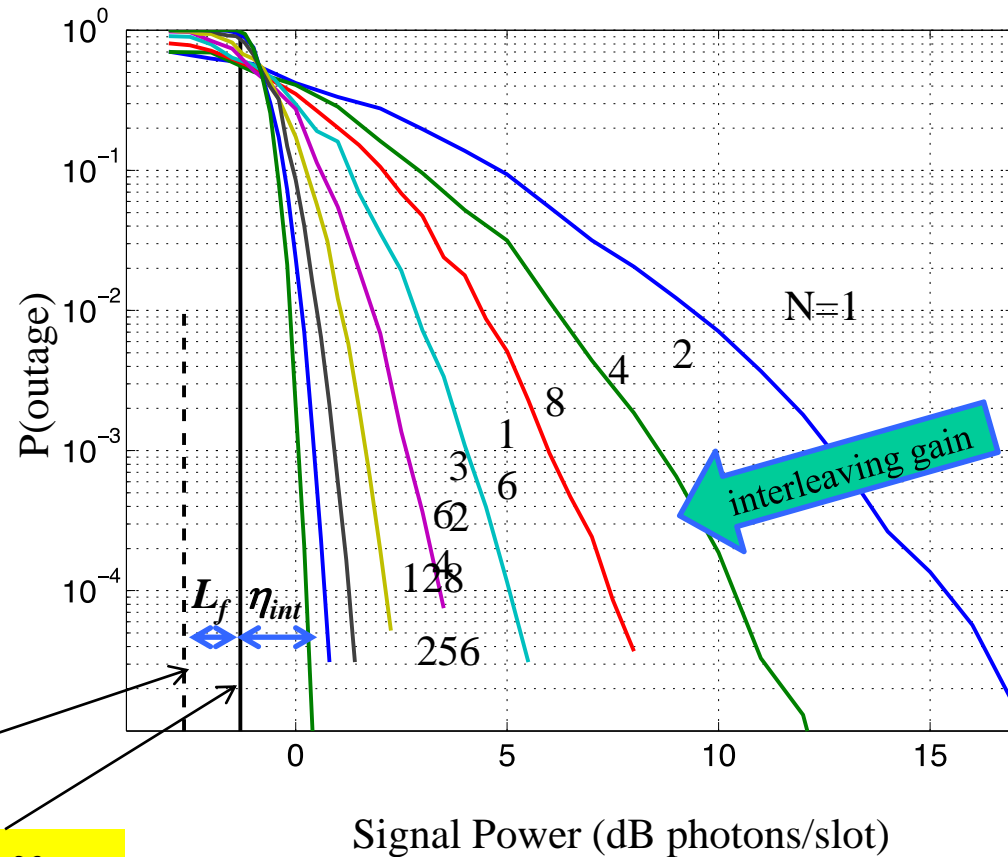
$$P(\text{outage}) = P\left(R > \bar{C} = \frac{1}{N} \sum_{i=1}^N C(v_i P)\right)$$

$$\bar{C} \xrightarrow{N \rightarrow \infty} C_f = \int C(vP) f_V(v) dv$$

Fading Capacity: Fundamental limit on performance in fading.

Fading capacity does not approach the capacity in the absence of fading. There is a loss due to fading dynamics, even with the same average received power.

The fading loss—the gap to the fading capacity, is nonrecoverable



Capacity Threshold (no fading)

$N \rightarrow \infty$
Fading Capacity Threshold

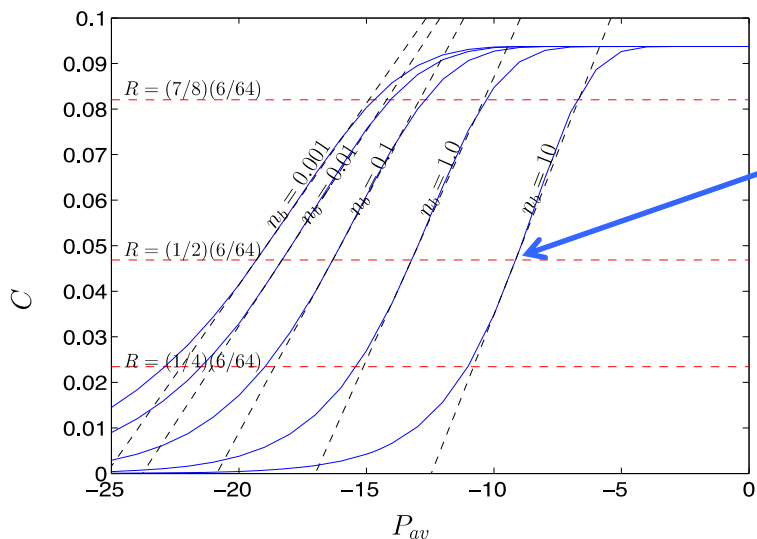
Divide loss into two terms:
 1. η_{int} = finite interleaver loss (recoverable)
 2. L_f = Fading Capacity Loss (not recoverable)



Analytic approximation of fading capacity loss

Capacity function is, in general, not known in closed form

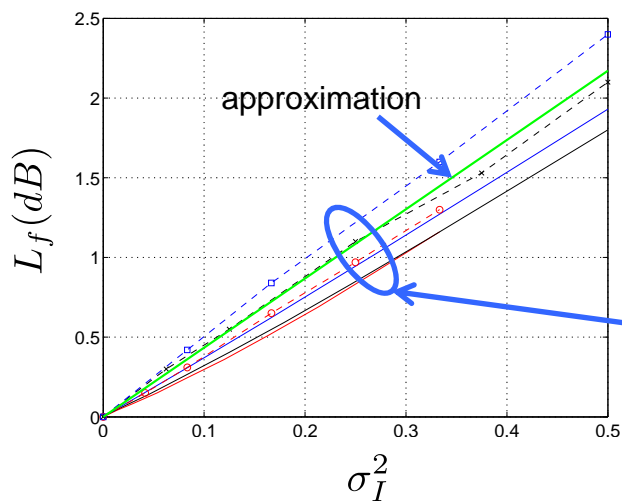
$$C_f = \int C(vP) f_V(v) dv$$



Linear approximation

$$C(P) \approx a \log(P) + \gamma$$

$$C_f(P) \approx C(P) - \frac{a}{2} \sigma_I^2$$



Numerically evaluated loss

$$L_f \approx R_{\text{ECC}} \sigma_I^2 \frac{10}{\ln(10)} \text{ dB}$$

dB Fading Capacity loss is linear in the scintillation index



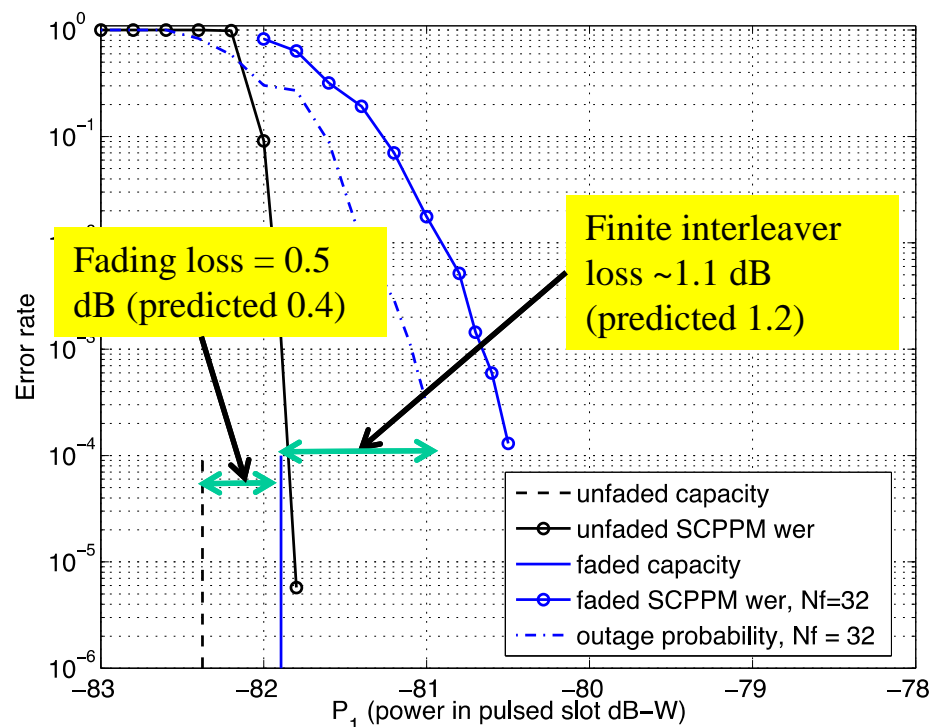
Analytic approximation of finite interleaver loss

$$P(\text{outage}) = P\left(R > \bar{C} = \frac{1}{N} \sum_{i=1}^N C(v_i P)\right)$$

$$\bar{C} = \frac{1}{N} \sum_{i=1}^N C(v_i P)$$

Approximate as Gaussian for large N, and apply linear approximation

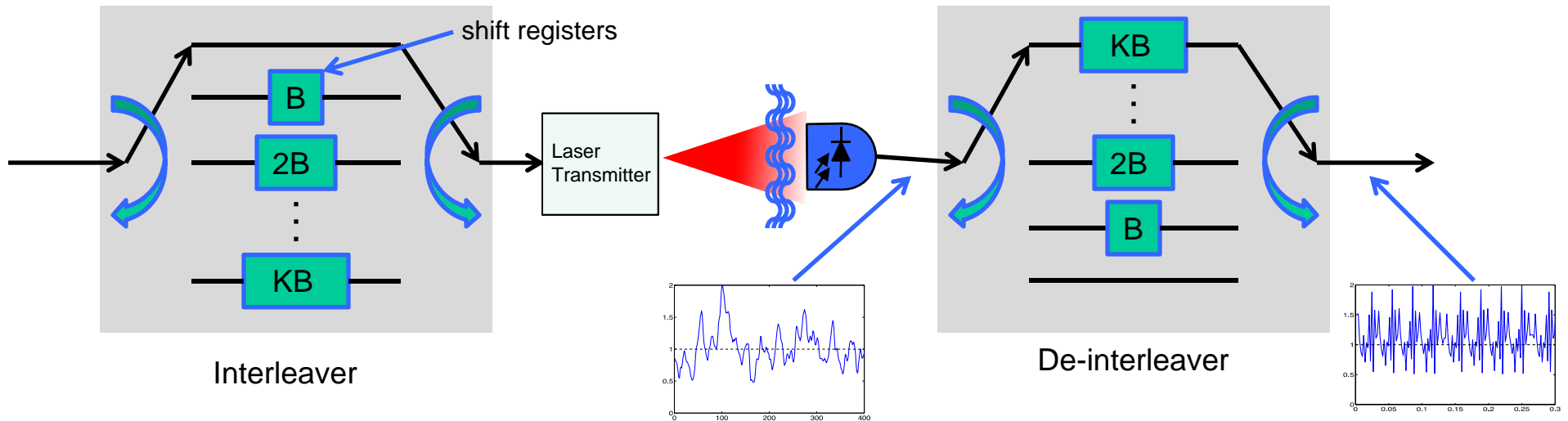
$$\eta_{int,dB} \approx 16 \frac{\sigma_I}{\sqrt{N_f}}$$



Interleaver Loss goes as the square root of the scintillation index

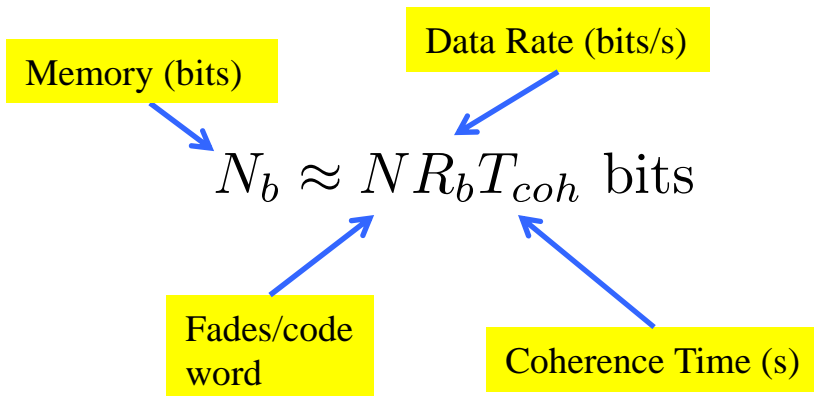


Interleaver memory requirements



- Convolutional interleaver achieves same spreading (N) as a block interleaver with half the memory

- Example: to achieve $N=100$, with $T_{coh}=10$ msec, $R_b=125$ Mbps, requires a 125 Mbit interleaver.



$$\eta_{int} \approx 16 \sqrt{\frac{\sigma_I^2 R_b T_{coh}}{N_b}} \text{ dB}$$



Conclusions

- **Free-space optical communication systems potentially gain many dBs over RF systems.**
- **There is no upper limit on the theoretically achievable photon efficiency when the system is quantum-noise-limited:**
 - Intensity modulations plus photon counting can achieve arbitrarily high photon efficiency, but with sub-optimal spectral efficiency.
 - Quantum-ideal number states can achieve the ultimate capacity in the limit of perfect transmissivity.
- **Appropriate error correction codes are needed to communicate reliably near the capacity limits.**
- **Poisson-modeled noises, detector losses, and atmospheric effects must all be accounted for:**
 - Theoretical models are used to analyze performance degradations.
 - Mitigation strategies derived from this analysis are applied to minimize these degradations.